(12)

David W. Taylor Naval Ship Research and Development Center

Bethesda, MD 20084-5000

DTNSRDC/SME-86-30 November 1986

Ship Materials and Engineering Department

Research and Development Report

FRACTURE ANALYSIS OF WELDED TYPE 304 STAINLESS STEEL PIPE

by

R.A. Hays

M.G. Vassilaros

J.P. Gudas

DTNSRDC/SME-86-30
FRACTURE ANALYSIS OF WELDED TYPE 304 STAINLESS STEEL PIPE

Approved for public release; distribution unlimited

MAJOR DTNSRDC TECHNICAL COMPONENTS

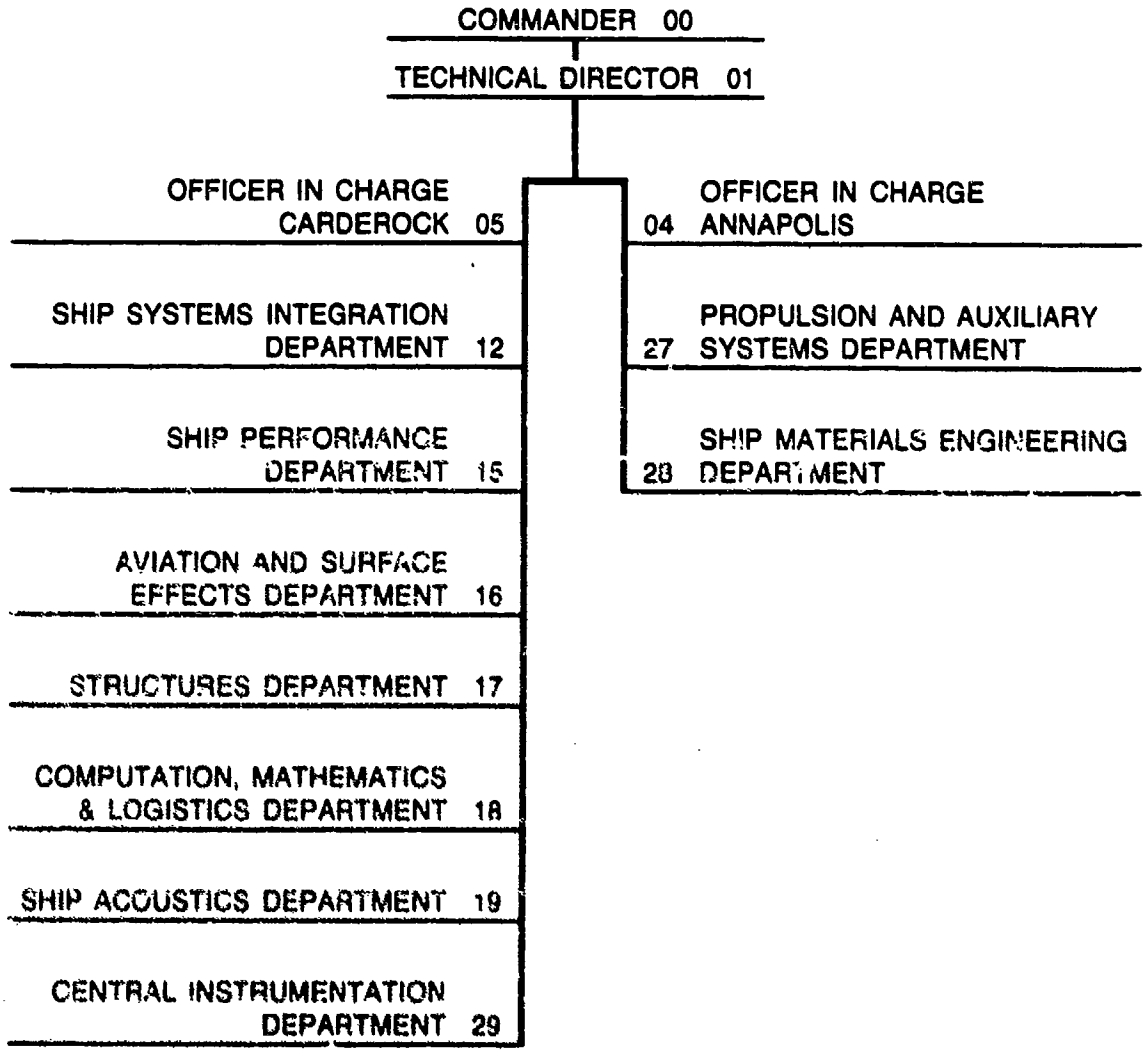

UNCLASSIFIED
SECURITY CLASSIFICATION OF THIS PAGE

REPORT DOCUMENTATION PAGE

AD-A176 294

1a. REPORT SECURITY CLASSIFICATION UNCLASSIFIED	1b RESTRICTIVE MARKINGS
2a. SECURITY CLASSIFICATION AUTHORITY	3. DISTRIBUTION/AVAILABILITY OF REPORT Approved for public release; distribution unlimited.
2b. DECLASSIFICATION/DOWNGRADING SCHEDULE	
4. PERFORMING ORGANIZATION REPORT NUMBER(S) DTNSRDC-SME-86-30	5. MONITORING ORGANIZATION REPORT NUMBER(S)
6a. NAME OF PERFORMING ORGANIZATION DTNSRDC	6b. OFFICE SYMBOL (If applicable) Code 2814
6c. ADDRESS (City, State, and ZIP Code) Bethesda, MD 20084-5000	7a. NAME OF MONITORING ORGANIZATION
8a. NAME OF FUNDING/SPONSORING ORGANIZATION U.S. Nuclear Regulatory Comm.	8b. OFFICE SYMBOL (If applicable)
8c. ADDRESS (City, State, and ZIP Code) Washington, DC 20555	7b. ADDRESS (City, State, and ZIP Code)
	9. PROCUREMENT INSTRUMENT IDENTIFICATION NUMBER
	10. SOURCE OF FUNDING NUMBERS PROGRAM ELEMENT NO. / PROJECT NO. / TASK NO / WORK UNIT ACCESSION NO. 1-2814-553

11. TITLE (Include Security Classification)

(U) FRACTURE ANALYSIS OF WELDED TYPE 304 STAINLESS STEEL PIPE

12. PERSONAL AUTHOR(S)
R.A. Hays, M.G. Vassilaros, J.P. Gudas

13a. TYPE OF REPORT	13b. TIME COVERED	14. DATE OF REPORT (Year, Month, Day)	15 PAGE COUNT
Final	FROM ____ TO ____	November 1986	53

16. SUPPLEMENTARY NOTATION

Prepared under Interagency Agreement RES-78-104

17. COSATI CODES			18. SUBJECT TERMS (Continue on reverse if necessary and identify by block number)
FIELD	GROUP	SUB-GROUP	Piping, stainless steel, J-integral, ASME Code, fracture mechanics.

19. ABSTRACT (Continue on reverse if necessary and identify by block number)

An experimental investigation was performed to determine the fracture resistance of 4 in. diameter circumferentially welded type 304 stainless pipe at 550°F (288°C). Two crack geometries were investigated. These were a circumferential through wall crack (simple) and circumferential through wall crack superimposed on a 360 degree radial crack on the inside diameter of the pipe (complex). Test results were analyzed using J-integral and limit load techniques. Additionally, J-integral resistance curve tests were performed on large plan-size compact tension specimens for comparison with the pipe specimen results.

Results of the J-integral analysis indicate that J-initiation for pipes containing simple cracks was approximately 1120 kJ/m^2 (6400 in-lb/in^2) and a factor of four decrease in J-initiation was noted for pipes containing the complex crack. Good agreement was shown at J-initiation between pipe specimens containing the simple crack geometry and compact tension specimens. The accuracy of the limit load analysis was variable for pipes containing the simple crack geometry with the average predicted limit load calculated using the ASME Code

20. DISTRIBUTION/AVAILABILITY OF ABSTRACT ☐ UNCLASSIFIED/UNLIMITED ☒ SAME AS RPT ☐ DTIC USERS	21 ABSTRACT SECURITY CLASSIFICATION UNCLASSIFIED
22a. NAME OF RESPONSIBLE INDIVIDUAL R.A. Hays	22b. TELEPHONE (Include Area Code) (301) 267-4986 / 22c. OFFICE SYMBOL Code 2814

DD FORM 1473, 84 MAR — 83 APR edition may be used until exhausted. All other editions are obsolete.

SECURITY CLASSIFICATION OF THIS PAGE

☆U.S. Government Printing Office 1986—626-612

Sq m Sq (in)

19. (continued)
flow stress being 8.7% higher than that actually attained in the tests. The calculated limit loads based on the ASME Code flow stress were conservative for the complex crack cases.

CONTENTS

CONTENTS (Continued)

FIGURES

FIGURES (Continued)

TABLES

ABBREVIATIONS

a	crack length in compact tension specimen
ASME	American Society of Mechanical Engineers
ASTM	American Society for Testing and Materials
DCPD	direct current potential drop
°C	degrees Centigrade
°F	degrees Fahrenheit
in.	inch
J-R	J-Integral Resistance
kg	kilogram
kJ	kilojoules
ksi	thousand pounds per square inch
lb	pound
MPa	megapascal
m	meter
mm	millimeter
NPS	nominal pipe size
W	compact tension specimen width

ABSTRACT

An experimental investigation was performed to determine the fracture resistance of 4 in. diameter circumferentially welded type 304 stainless pipe at 550°F (288°C). Two crack geometries were investigated. These were a circumferential through wall crack (simple) and circumferential through wall crack superimposed on a 360 degree radial crack on the inside diameter of the pipe (complex). Test results were analyzed using J-integral and limit load techniques. Additionally, J-integral resistance curve tests were performed on large plan-size compact tension specimens for comparison with the pipe specimen results.

Results of the J-integral analysis indicate that J-initiation for pipes containing simple cracks was approximately 1120 kJ/m^2 (6400 $in\text{-}lb/in^2$) and a factor of four decrease in J-initiation was noted for pipes containing the complex crack. Good agreement was shown at J-initiation between pipe specimens containing the simple crack geometry and compact tension specimens. The accuracy of the limit load analysis was variable for pipes containing the simple crack geometry with the average predicted limit load calculated using the ASME Code flow stress being 8.7% higher than that actually attained in the tests. The calculated limit loads based on the ASME Code flow stress were conservative for the complex crack cases.

ADMINISTRATIVE INFORMATION

This study was sponsored by the U.S. Nuclear Regulatory Commission and was performed under Interagency Agreement RES-78-104, Modification 8, DTNSRDC Work Unit Number 1-2814-553-90. Mr. Milton Vagins and Mr. Jack Strosnider, Materials Engineering Branch, Office of Nuclear Regulatory Research, have been project officers during the course of this research.

INTRODUCTION

The fracture resistance of type 304 stainless steel piping is of concern in the nuclear power industry due to the potential presence of stress corrosion cracks associated with weldments in this material. Because of the high toughness of reactor piping materials and the large amount of plastic deformation

and crack growth which occurs prior to fracture instability, linear elastic fracture mechanics procedures for assessing fracture safety are felt to be unnecessarily conservative. However, a relatively simple safety analysis is desirable.

The objectives of this investigation were threefold. The primary objective was to evaluate the fracture toughness of welded type 304 stainless steel pipe. The second objective was to evaluate the applicability of using compact tension specimens to model the pipe fracture behavior. This is important due to the relatively high cost of full scale pipe fracture experiments. Lastly, the full scale pipe fracture tests were evaluated using the limit load technique prescribed in the American Society of Mechanical Engineers (ASME) Boiler and Pressure Vessel Code.

In order to accomplish these objectives, a series of seven full-scale pipe fracture experiments on circumferentially welded, 4-in. nominal pipe size (NPS) (mean diameter 106 mm) schedule 80, type 304 stainless steel pipe, and a series of of five fracture experiments on compact tension specimens were performed. The compact specimens ranged in plan size from 1T to 3T with the thickness dimension the same as the pipe wall thickness.

BACKGROUND

Fracture experiments on full-scale pipe specimens have been conducted by several investigators.[1-3] An apparent geometry dependence of the J-integral resistance (J-R) curve obtained from full-scale tests was reported by Wilkowski, et al.[1] In this work, J-R curves obtained from two types of laboratory specimens, the center cracked panel and the three-point bend specimen, were compared with J-R curves obtained from 4-in. NPS pipes containing circumferential through-wall notches and loaded in four-point bending. The authors cited a dependence of the J-R curve on the degree of constraint at the crack tip and attributed the differences in results obtained from the different types of specimens to this dependence.

Vassilaros, et al.[2] obtained relatively good agreement between full-scale pipe fracture experiments and laboratory sized compact tension specimens for a ferritic piping steel. In this case, the compact specimens were cut directly from the wall of the 8 in. NPS pipe of the same type that was used in the fracture experiments. This limited the maximum size of the compact specimens to 1T plan. Larger 2T plan specimens were also used in this work but the specimen blanks had to be flattened prior to testing and were found to yield results inapplicable to the pipe specimens. Due to the relatively small size of the 1T and 2T plan compact specimens, the J-R curve results were comparable over a very small range of crack extension.

The ASME Code, Section XI IWB-3640[4] gives guidance for the evaluation of pipe flaws in austenitic stainless steel piping and associated nonflux weldments. The failure criterion due to Ranganath, et al.[5] is based on net section collapse. This criterion has been shown to be effective in predicting failure of stainless steel pipes containing circumferential cracks.[6,7]

MATERIALS

The full-scale pipe fracture experiments were performed on 4-in. NPS (mean diameter 101.6 mm) schedule 80, circumferentially welded SA-312 type 304 stainless steel pipe sections with an overall length of approximately 1219 mm (48 in.). The pipes were welded at Battelle's Pacific Northwest Laboratories using an automatic gas tungsten arc welding procedure. The edge preparation was single "V" and the average heat input was 1.18 kJ/mm (30 kJ/in.). Due to the small diameter of the pipe, the compact and tensile specimens were machined from 914.4-mm (36-in.) long by 8.64-mm (0.34-in.) thick plates welded using nominally the same procedure and heat input in order to approximate the pipe tensile and fracture properties. The edge preparation was double "V".

The tensile properties of the base and weld material at 288°C (550°F) were measured at Battelle's Columbus Division and are given in Table 1. The base metal tensile specimens were oriented with the long axis in the direction of the weld length. The weld metal specimens were machined in the same orientation and made entirely of weld metal. It can be seen from the table that the weld metal had a yield strength approximately twice that of the base metal and a flow stress (calculated as the average of the yield and ultimate streugths) approximately 62 MPa 9 ksi) greater than the base metal. The materials exhibited similar tensile ductility properties.

EXPERIMENTAL PROCEDURE

PIPE SPECIMEN TESTS

The full-scale pipe fracture specimens were loaded in four-point bending using a 1.33 Mn (300,000 lb) capacity screw type testing machine under displacement control in a manner similar to that of Vassilaros, et al.[2] Figure 1 gives a schematic of the loading configuration. Five channels of data were taken during the experiments including load, cross-head deflection, load line displacement, crack mouth opening displacement, and electrical potential drop across the crack mouth. All of the data were stored in digital form on magnetic media. Two crack configurations were tested as shown in Fig. 2. The first was a through wall crack growing circumferentially (simple) and the second was a through wall crack superimposed on a 360 degree interior radial flaw (complex). The flaws were machined such that they were contained entirely within the weld metal and were sharpened in fatigue prior to testing. A total of seven pipe tests were conducted. Five tests were conducted in a noncompliant test rig and two were conducted in a test rig made compliant using springs in series with the load train. The J-integral analysis was performed for

the five pipes tested in the noncompliant test rig while the limit load analysis was performed on all pipe specimens. The complete pipe test matrix is given in Table 2.

Crack extension during the tests was monitored using elastic compliance and DC potential drop (DCPD) techniques simultaneously. The elastic compliance technique used the slope of the load versus crack mouth opening displacement curve obtained during small elastic unloadings performed periodically during the tests. The specimen compliance was then compared to a compliance calibration curve to predict crack extension. The calibration curve used initially was that of Joyce[8] which was constructed using results from 4-in. NPS aluminum pipe. However, during loading and subsequent crack growth in the stainless steel pipe tests, ovalization of the crack cross-section similar to that observed by Bruckner, et al.[3] occurred with the vertical diameter of the cross-section becoming longer and the horizontal diameter becoming shorter. This ovalization produced a stiffening of the New calibration curves were constructed using the measured initial and final crack lengths and the measured specimen compliances for both crack geometries. Figure 3 compares the compliance calibrations used for the pipes with that of Reference [8]. The curve used for the pipe specimens containing simple flaw geometries has a lower slope than the other two curves on the figure. This indicates that when crack cross-section ovalization takes place, a real increase in specimen compliance corresponds to a larger increase in crack length than when the crack cross-section remains circular. Because of the presence of the radial flaw in the pipes containing complex crack geometry, very little cross-section ovalization took place during the tests. Thus the compliance calibration curve for the complex crack case appears very similar to that of Joyce.[8]

Table 1. Base and weld metal tensile properties at 288°C (550°F).

	YIELD STRENGTH MPa (ksi)	ULTIMATE STRENGTH MPa (ksi)	FLOW STRESS MPa (ksi)	% ELONG (IN 1 in.)	% RED. IN AREA
WELD	306 (44.3)	451 (65.4)	379 (54.9)	33	74.3
	291 (42.2)	443 (64.3)	368 (53.3)	30	72.9
AVG	299 (43.3)	447 (64.8)	373 (54.1)	31.5	73.6
BASE	153 (22.2)	464 (67.3)	309 (44.8)	39.0	70.8
	157 (22.8)	474 (68.8)	316 (45.8)	40.5	70.8
AVG	155 (22.5)	469 (68.1)	312 (45.3)	39.8	70.8

Table 2. Pipe specimen test matrix.

Pipe ID	Crack Geom.	Init. Crack Angle, 2 deg.	Outer Span Length, L mm (in.)	Inner Span Length, S mm (in.)	Mean Radius, R mm (in.)	Wall thickness, t mm (in.)	Radial Crack Length, a mm (in.)	a/t
GAM-100		100	1067 (42)	381 (15)	52.8 (2.08)	8.64 (0.34)	-	-
GAM-200		139	1067 (42)	381 (15)	52.8 (2.08)	8.64 (0.34)	-	-
GAM-700*	Simple	96.3	1067 (42)	381 (15)	52.8 (2.08)	8.64 (0.34)	-	-
GAM-800*		118	1067 (42)	381 (15)	52.8 (2.08)	8.13 (0.32)	-	-
GAM-900		107	1067 (42)	381 (15)	52.8 (2.08)	8.26 (0.33)	-	-
GAM-400	Complex	154	1067 (42)	381 (15)	54.6 (2.15)	8.64 (0.34)	3.28 (0.129)	0.380
GAM-600		128	1067 (42)	381 (15)	52.8 (2.08)	8.38 (0.33)	2.21 (0.087)	0.256

* Compliant test

The DCPD technique used was similar to that described by Vassilaros and Hackett[9] except that the relationship between crack length and potential drop after blunting was obtained by fitting an exponential equation to the data of Wilkowski and Maxey.[10] After each test the specimens were heat tinted and broken open. The initial and final crack lengths were then measured at the inner and outer diameter as well as on several points along the pipe radius. These average initial and final crack lengths were reported and used in the DCPD analysis.

Due to the sparseness of the crack length data near crack initiation, J-initiation was calculated for the pipe specimens as the intersection between the blunting line and a straight line fit to all data after crack initiation. As compared with the ASTM E813 standard for laboratory bend and compact specimens, the straight line fit places more emphasis on points with large crack extension and tends to yield higher J-initiation points.

COMPACT SPECIMEN TESTS

A series of five J-R curve tests were performed at 288°C (550°F) on modified compact tension specimens with 1T, 2T, and 3T plan geometries. The specimens blanks were cut from the welded plate and machined to a thickness of 8.64 mm (0.34 in.) which corresponds to the nominal pipe wall thickness. The notches were machined such that they were contained entirely within the weld and crack growth occurred in the direction of the weld. A schematic of the specimen design is shown in Fig. 4 and a test matrix is given in Table 3. All specimen measurement and preparation procedures detailed in ASTM E813-81 were followed in this phase of testing. Specimens were precracked to an approximate 0.65 a/W where a is the crack length and W is the specimen width.

Table 3. Compact tension specimen test matrix.

Plan Size	No. of Specimens	W mm (in.)	B mm (in.)	a mm (in.)	a/W	B/b
3T	1	152 (6.00)	8.60 (0.34)	99.1 (3.90)	0.65	0.162
2T	2	102 (4.00)	8.60 (0.34)	66.0 (2.60)	0.65	0.242
1T	3	50.8 (2.00)	8.60 (0.34)	33.0 (1.30)	0.65	0.486

Methods of estimating crack length used during testing of the compact specimens were similar to those used for the pipe specimens. The computer interactive single specimen elastic compliance technique introduced by Joyce and Gudas[11] was used as well as the DCPD technique described by Vassilaros and Hackett.[9] However, due to the high curvature of the crack opening displacement versus potential drop curve, maximum load was used as the criteria for crack initiation. The J-integral values calculated for the compact specimens used the crack growth corrected deformation J expression published by Ernst, Paris, and Landes.[12] J-initiation values were calculated using the standard ASTM E813-81 procedure.

PIPE SPECIMEN ANALYSES

J-INTEGRAL RESISTANCE CURVE ANALYSIS

This investigation included an evaluation of the critical J for initiation of of ductile fracture in the welded pipe and compact specimens and a comparison of the J-R curves from both types of specimens. J-integral values were calculated using an expression published by Zahoor and Kanninen.[13] This formulation requires actual load line displacement and bending moment data as inputs thus accounting for material hardening during loading. The J-integral expression, which also has a crack growth component, is as follows:

$$J = K^2/E + \beta \int_{\delta_0}^{\delta} (2P)\, d\delta + \int_{\phi_0}^{\phi} \gamma\, J\, d\phi \qquad (1)$$

where

K = stress intensity factor;

E = elastic modulus;

$\beta = -h'(\phi)/Rt\ h\ (\phi)$

2P = Total Bending Load

δ = plastic load line deflection

γ = $h''(\phi)/h'(\phi)$

R = radius

t = thickness

ϕ = total crack angle

$h(\phi)$ = [cos ($\phi/4$) - 1/2 Sin ($\phi/2$)]

LIMIT LOAD ANALYSIS

The limit load or net section collapse approach assumes that the remaining ligament of the crack cross section forms a plastic hinge and that failure occurs at a critical value of stress called the flow stress. Neglecting the stresses due to internal pressure, the limit moment given by reference [14] (see Fig. 5):

$$M_p = 4\sigma_o R^2 \, t \, \overline{M}_p \, (\theta, a) \qquad (2)$$

where

σ_o = material flow stress
R = mean pipe radius
t = mean wall thickness
θ = half crack angle
$\overline{a}$ = radial crack depth/mean wall thickness

and

$$\overline{M}_p = (1-\overline{a})(\cos\theta/2 - \frac{1}{2}\sin\theta), \text{ assuming no crack closure} \qquad (3)$$

or

$$\overline{M}_p = (1-\overline{a}) \left[\left(\frac{1-\overline{a}}{2} \right) \cos\theta/2 - \frac{1}{2}\sin\theta \right], \text{ assuming crack closure.} \qquad (4)$$

It is unlikely that closure of the radial crack on the compressive side of the neutral axis occurred due to the machining process required to produce the complex crack geometry.

A screening criteria for the application of the limit load analysis for pipes has been developed by Wilkowski, et al.[15] According to this reference, a limit load analysis is applicable for circumferential cracks if the length of the plastic zone preceding the crack tip is greater than or equal to the distance from the initial crack tip to the neutral axis, that is:

$$\left(\frac{EJ_{Ic}}{\pi\sigma^2}\right) \Big/ \left(\frac{\pi - \alpha}{4}\right) D \qquad (5)$$

where

E = elastic modulus
J_{Ic} = material fracture toughness from bend specimen
σ_o = material flow stress
D = mean pipe diameter
α = half crack angle in radians

While the numerator may not be an accurate estimate of the plastic zone size for a pipe, empirical evidence suggests that a comparison of toughness, strength, and crack size can be used to evaluate the applicability of a limit load analysis. The values of this ratio was approximately 13 for the welded type 304 stainless steel pipe specimens indicating that a limit load analysis should be applicable.

PIPE J-INTEGRAL RESISTANCE CURVE RESULTS

SIMPLE CRACK GEOMETRY PIPE SPECIMEN RESULTS

J-R curve results for pipe specimen GAM-100 which contained a simple through-wall flaw are given in Fig. 6. Although elastic compliance and DCPD techniques were used simultaneously to estimate crack lengths during the tests, elastic compliance data only is available for this specimen. This figure presents J versus average crack extension data for one crack tip. The filled symbol indicates the average optically measured crack length. As can be seen from the figure, the elastic compliance technique over-predicted the measured final crack length by

approximately 7%. During the test, both crack tips remained within the weld metal. An approximate J-initiation level of 822 kJ/m^2 (4700 in-lb/$in.^2$) was measured for this specimen.

J-R curve results for pipe specimen GAM-200 are given in Fig. 7. Both elastic compliance and DCPD results were obtained for this test. Again, the elastic compliance technique over-predicted the final crack length by a small margin. The optically measured initial and final crack lengths are used in DCPD analysis thereby precluding over-estimation or under-estimation. The elastic compliance results yielded a lower estimate of J-initiation and a lower resistance curve slope than the DCPD technique for this test. The J-initiation results were 962 kJ/m^2 (5500 in-lb/$in.^2$) and 1068 kJ/m^2 (6100 in-lb/$in.^2$) for the elastic compliance and DCPD techniques respectively.

Elastic compliance and DCPD results were also obtained for pipe specimen GAM-900 and are shown in Fig. 8. J-initiation values for this specimen from the elastic compliance and DCPD techniques were 1595 kJ/m^2 (9117 in-lb/ $in.^2$) and 1150 kJ/m^2 (6575 in-lb/$in.^2$), respectively. In this test the elastic compliance technique under-predicted the final measured crack length by approximately 15% leading to an artificially high J-R curve. Notable in this figure is that the elastic compliance technique produced a higher J-initiation level and a lower resistance curve slope than did the DCPD technique. The high prediction of J-initiation relative to that predicted by DCPD may be due to the insensitivity of the elastic compliance technique to crack initiation at short initial crack lengths as a result of the large distortions in the crack cross-section and overall plasticity in the region near the crack.

Figure 9 presents a comparison of the J-R curves for the pipes with the simple crack geometry. Good agreement in overall J-R curve behavior between pipe specimens GAM-100 and GAM-200 is shown with pipe specimen GAM-900 being considerably above these two results. This difference in toughness is also reflected in the amount of ovalization which occurred during the tests. Pipe specimens GAM-100 and GAM-200 had changes in vertical diameter of 3% and 2% respectively while specimen GAM-900 had a change in vertical diameter of 6%. A comparison of the DCPD J-R curve results in Fig. 10 shows good agreement at J-initiation for pipe specimens GAM-200 and GAM-900. The difference in resistance curve slopes may be due to the difference in initial crack lengths as suggested by Smith.[16] The range of initiation toughnesses measured here agree to a large extent with those measured for 4 in. NPS base metal type 304 stainless steel pipes in Reference [1]. This result indicates that the presence of the overmatching circumferential weld does not affect the initiation toughness of the pipe to a large degree.

COMPLEX CRACK GEOMETRY PIPE SPECIMEN RESULTS

J-R curve results for pipe specimen GAM-400 which contained a complex crack geometry are given in Fig. 11. Elastic compliance and DCPD data agree very well for this specimen. The long initial crack angle ($2\theta = 154°$) and nearly 40% through-wall radial crack reduced specimen distortion and kept the crack plane perpindicular to the long axis of the pipe contributing to the repeatability of the J-R curve measurement. J-initiation for this specimen was approximately 262 kJ/m^2 (1500 in-lb/in.^{2}).

J-R curve results from DCPD for pipe specimen GAM-600 which had an initial crack angle $2\theta = 128°$ and a radial crack depth of 25% of the wall thickness are shown in Fig. 12. These results indicate a J-initiation value of approximately 228 kJ/m^2 (1300 in-lb/$in.^2$) and a high resistance curve slope as compared with results from pipe specimen GAM-400. This difference in slope is evident in Fig. 13 where results from the two specimens are plotted together. The shorter initial circumferential and radial crack lengths in specimen GAM-600 produced higher loads and more general yielding away from the crack cross-section. The technique used to measure the amount of energy applied to the specimen cannot make a distinction between that applied to the crack tip and that being used to deform the base metal, accounting for the difference in resistance curve slopes between the two specimens.

COMPARISON OF SIMPLE AND COMPLEX CRACK GEOMETRY RESULTS

Comparison of test results from the pipes containing the two crack geometries reveals a significant lowering in fracture toughness from the pipes with the simple crack geometry to the pipes with the complex crack geometry. Representative J-R curves for pipes containing the two crack geometries from elastic compliance and DCPD data are plotted in Figs. 14 and 15 respectively. The data in Fig. 14 indicate a decrease in initiation toughness by a factor of approximately 3 and a clear reduction in resistance curve slope between the pipes containing simple and complex cracks. This is expected due to the high level of constraint imposed by the complex crack geometry and the 38% reduction in wall thickness. The data in Fig. 15 support the large reduction in initiation toughness showing a reduction of approximately 5-1/2 between pipes containing different crack geometries. Again there is a reduction in resistance curve slope. However, it is not as large as the data shown in the previous figure. This is a result of the pipe containing the complex crack only having a 25% reduction in wall thickness.

The decrease in toughness between the pipes containing the simple and complex cracks is also evident from the load versus displacement records. Figure 16 gives representative curves from pipes containing the two types of crack geometry. The simple crack geometry is characterized by a rather flat curve both before and after maximum load. The complex crack geometry is characterized by attainment of maximum load very early in terms of displacement and a large negative slope after maximum load.

COMPACT TENSION SPECIMEN J-INTEGRAL RESISTANCE CURVE RESULTS

ELASTIC COMPLIANCE RESULTS

Both elastic compliance and DCPD techniques were used to estimate crack extension for the compact tension specimens as well as the pipe specimens. Figure 17 presents the J-R curve results from the 1T and 2T plan specimens produced using the elastic compliance technique. There is considerable variability in the curves with the J-initiation values ranging from 840 kJ/m^2 (4800 $in\text{-}lb/in.^2$) to 1400 kJ/m^2 (8000 $in\text{-}lb/in.^2$). The figure shows that the 1T plan specimen GGP-1 produced the lowest curve of the four specimens reported. The elastic compliance technique predicted the final crack length within 5% for this specimen while under-predicting the final crack lengths of the other three specimens by an average of 30%. Correcting the J-R curves of these three specimens to meet the final crack length would produce lower curves and better agreement with the results from specimen GGP-1.

DC POTENTIAL DROP RESULTS

The variability in J-R curves from the compact specimens discussed above was reduced considerably when the DCPD data was analyzed since this analysis is tied to the measured initial and final crack lengths. This is evident in Fig. 18 which

is a plot of the J-R curve results from the 1T, 2T, and 3T plan specimens. J-initiation values range from approximately 858 kJ/m^2 (4900 in-lb/$in.^2$) to 1120 kJ/m^2 (6400 in-lb/$in.^2$) for these curves. It appears from this data that there is no significant J-R curve dependence on specimen plan size.

COMPARABILITY OF PIPE AND COMPACT SPECIMEN J-INTEGRAL RESISTANCE CURVE RESULTS

An important aspect of the work presented here is the use of laboratory-sized compact tension specimens to model the J-R curve behavior of the larger and considerably more expensive full-scale pipe specimens. In this investigation, pipes with simple through-wall circumferential cracks were modeled using nonside grooved specimens of varying plan size with the thickness dimension the same as the nominal pipe wall thickness. The range of J-R curve results from elastic compliance data for both specimen types are plotted in Fig. 19. It appears from this figure that the compact specimen data validates the highest of the resistance curves from the pipe specimens. However, difference in weld geometry and the inability of the elastic compliance technique to accurately predict the final crack length for either the pipe or compact specimens leads to some uncertainty in the results. As stated above, correction for under-prediction of the measured final crack length leads to lowering of the J-R curve after crack initiation.

Figure 20 presents the range of J-R curve results from DCPD data for the pipe and compact specimens. The good agreement in initiation toughness between the two types of specimens can be seen from this figure. Comparison of resistance curve slopes is very difficult here due to the small amount of crack extension which occurred in the compact specimens and the sparsity of the pipe crack extension data in the small crack extension region. It does appear, however, that the compact specimens show a higher initial slope than the pipe specimens. Far field slopes appear comparable between the two types of specimens.

PIPE LIMIT LOAD ANALYSIS RESULTS

Because crack initiation occurred prior to maximum load and in some cases the crack tips grew out of the weld and into the base metal, the limit load analyses were performed using three different flow stresses. The first was the ASME Code 3 Sm flow stress for type 304 stainless steel at 288°C (550°F). That value is 352 MPa (51.0 ksi). The second and third were calculated as the average of the yield and ultimate strengths measured at 288°C (550°F) on the weld and base metals respectively. These values were measured using tensile specimens cut from the welded plate used for the compact specimens and are 373 MPa (54.1 ksi) and 312 MPa (45.3 ksi) for the weld metal and base metal respectively.

SIMPLE CRACK GEOMETRY PIPE SPECIMEN RESULTS

The results for specimen GAM-100 indicate that the limit load analysis was nonconservative in that the predicted load carrying capacity calculated using the limit load analysis was higher than that actually achieved during testing for all the flow stress values. Although both crack tips stayed in the weld metal as stated above, it may still be proper to apply the limit load calculated using the base metal materials property data. This is justified due to the large amount of yielding that occurred in the base metal. Results for all five simple crack geometry pipes are given in Table 4. Figure 21 presents the test results and limit load analyses from specimen GAM-200. The three horizontal lines on the figure correspond to the limit loads calculated using the three different flow stress values. Both crack tips grew out of the weld metal and into the base metal during this test and extensive base metal plasticity occurred indicating that the limit load should be calculated based on the base metal flow stress. Using this value, the predicted limit load was conservative by 8%. It should be noted that the limit load calculated using the ASME Code flow stress value predicted that actually attained by the pipe

within 3%. Figure 22 presents results from another specimen (GAM-900) which shows very good agreement between the predicted limit load calculated using the ASME Code flow stress and the actual maximum load. The predicted load calculated using the weld metal materials property data is 4.4% nonconservative. While the predicted load calculated using the base metal materials property data was 11.6% conservative.

The limit load calculated using the ASME Code flow stress was the most consistent predictor of actual maximum load. However, the limit load predicted using the ASME Code flow stress was 8.7% higher on average than that attained by the pipe specimens during testing. The limit load predicted using the base metal materials property data was an average of 3% lower than that attained by the pipe specimens.

COMPLEX CRACK GEOMETRY PIPE SPECIMEN RESULTS

Since all crack extension in the complex crack geometry pipe tests occurred in the weld metal, these tests were analyzed using the ASME Code and weld metal materials property data flow stresses only. The load versus deflection record for pipe GAM-600 which contained the complex crack geometry is given in Fig. 23 with the two calculated limit loads. These loads were calculated assuming closure of the radial crack on the compressive side of the neutral axis did not occur. In this case the actual maximum load fell between the two predicted limit loads. Results for both pipes tested with the complex crack geometry are given in Table 4. Results for pipe specimen GAM-400 are clearly conservative. This may be due to the relatively long initial crack length as well as the considerable skewing of the crack front which took place during fatigue precracking. The technique used to measure initial crack lengths (linear averaging of crack length across the wall thickness) may have placed too much emphasis on the longer internal crack. Were this the case, the measured crack length input into the limit load expression would be longer than the effective crack length resulting in a lower prediction of load carrying capacity.

Table 4. Pipe specimen limit load summary.

(simple crack geometry)

Pipe ID	Flow Stress MPa (ksi)	Maximum Load kN (lb)	Limit Load kN (lb)	$\left(\frac{P_{max}-P_{Lim}}{P_{max}}\right)100$
GAM-100	352(a) (51.0)	77.0 (17300)	93.0 (20900)	-20.8
	373(b) (54.1)		98.7 (22200)	-28.8
	312(c) (45.3)		82.7 (18600)	-7.5
GAM-200	352(a) (51.0)	60.9 (13700)	62.7 (14100)	-2.9
	373(b) (54.1)		66.7 (15000)	-9.5
	312(c) (45.3)		55.6 (12500)	8.0
GAM-700	352(a) (51.0)	79.6 (17900)	96.1 (21600)	-20.7
	373(b) (54.1)		102 (22900)	-27.9
	312(c) (45.3)		85.4 (19200)	-7.3
GAM-800	352(a) (51.0)	73.4 (16500)	73.8 (16640)	-0.85
	373(b) (54.1)		78.3 (17650)	-6.9
	312(c) (45.3)		65.8 (14800)	10.3
GAM-900	352(a) (51.0)	84.1 (18900)	82.7 (18600)	1.6
	373(b) (54.1)		87.6 (19730)	-4.4
	312(c) (45.3)		74.3 (16700)	11.6

(complex crack geometry)

Pipe ID	Flow Stress MPa (ksi)	Maximum Load kN (lb)	Limit Load kN (lb)	$\left(\frac{P_{max}-P_{Lim}}{P_{max}}\right)100$
GAM-400	352(a) (51.0)	41.8 (9400)	33.4 (7500)	20.9
	373(b) (54.1)		35.1 (7900)	16.5
GAM-600	352(a) (51.0)	53.2 (11950)	50.7 (11380)	4.9
	373(b) (54.1)		53.8 (12075)	-1.0

(a) 3Sm
(b) Average of Weld Metal Yield and Tensile Strengths
(c) Average of Base Metal Yield and Tensile Strengths

CONCLUSIONS

An experimental investigation was performed to determine the fracture toughness of full-size welded 4-in. NPS type 304 stainless steel pipe with simple and complex crack geometries. Compact laboratory specimens of the same thickness as the pipe wall were also used to model the fracture behavior of the pipes containing the simple crack geometry. Results of the pipe fracture toughness experiments were analyzed using the value of the J-integral at crack initiation and a qualitative comparison of the J-R curves. Additionally, a limit load analysis was performed for all pipe specimens. Several conclusions can be drawn from the results of this investigation:

1. Crack initiation for welded type 304 stainless steel pipe containing simple through-wall circumferential cracks occurred at a J level of approximately 1120 kJ/m^2 (6400 in-lb/in.^{2}).

2. Increased crack tip constraint due to the presence of the internal notch in the complex crack geometry reduced the J level at crack initiation by approximately a factor of four as compared to the simple crack geometry.

3. Ovalization of the crack cross-section and large amounts of plasticity in the near-crack region lead to uncertainty in elastic compliance and DC potential drop crack length estimation techniques respectively.

4. Crack initiation for compact specimens occurred at an average J level of 1050 kJ/m^2 (6000 in-lb/in.^{2}).

5. Good agreement between the pipe and compact specimens using the DC potential drop technique indicates that crack initiation toughness measurements on laboratory-size specimens may be applicable to pipe geometries.

6. The accuracy of the limit load analysis was variable for the pipes containing the simple crack geometry. The limit load calculated using the ASME Code 3 Sm

flow stress was the most consistent predictor of maximum load of the three flow stresses used, but was an average of 8.7% nonconservative.

7. In some cases the cracks grew out of the weld metal and into the base metal during the tests. In these cases, better agreement was seen between the maximum load and the limit load calculated using the base metal materials property data.

8. The limit load analysis was a much more conservative predictor of maximum load for the pipes containing the complex crack geometry. The actual maximum load attained in both tests was greater than the limit load calculated using the ASME 3Sm flow stress.

ACKNOWLEDGEMENTS

The authors wish to thank Messrs. Jack Strosnider and Milton Vagins of the U.S. Nuclear Regulatory Commission for their support during the course of this research. The authors would also like to acknowledge the support of those at David Taylor Naval Ship R&D Center who contributed to this work, especially Mr. Paul Ditta. The advice and guidance of Dr. James Joyce of the U.S. Naval Academy and Mr. Gery Wilkowski of Battelle Columbus Laboratories is also gratefully acknowledged.

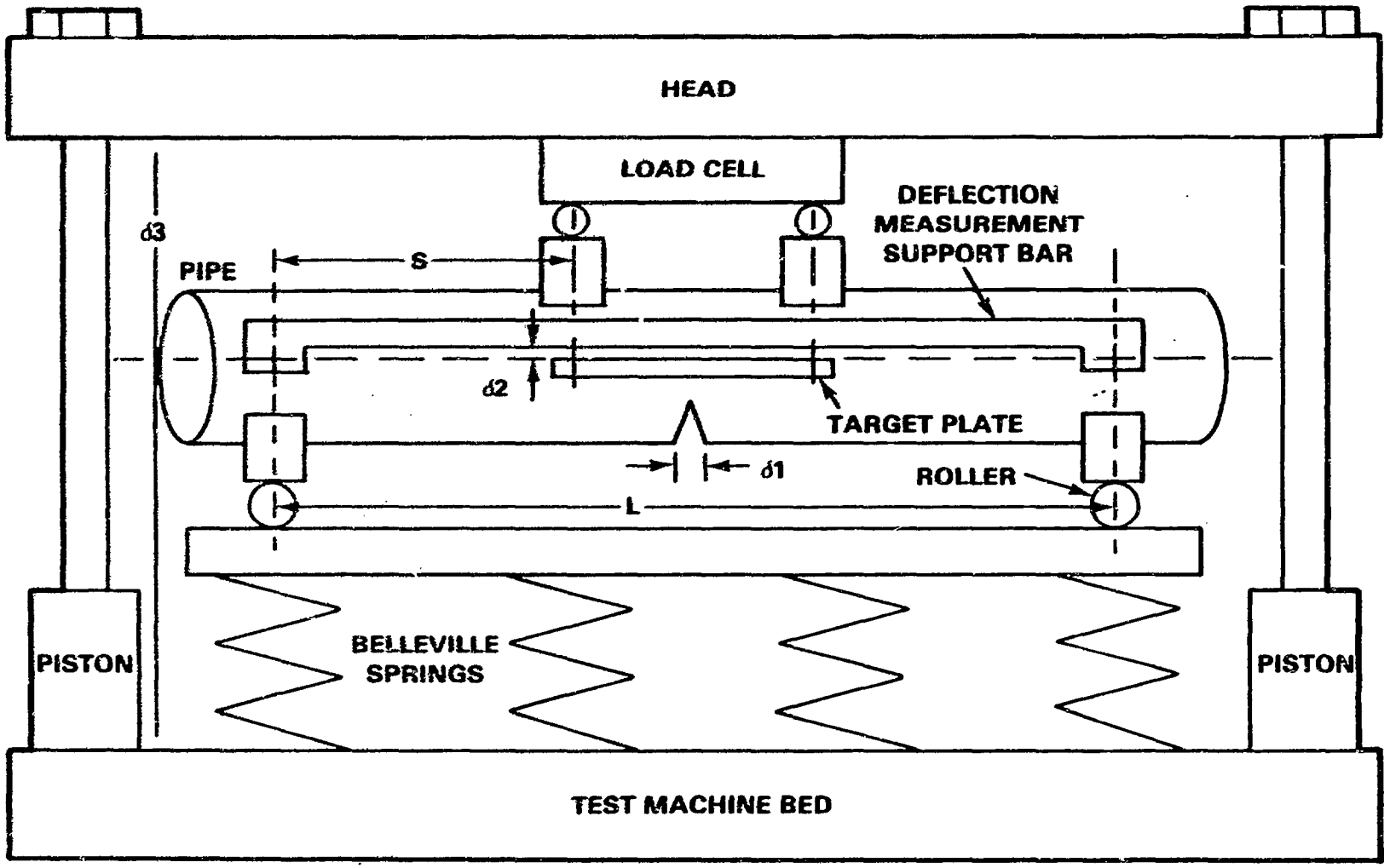

δ1 = CRACK MOUTH OPENING DISPLACEMENT
δ2 = PIPE LOAD LINE DEFLECTION
δ3 = TOTAL DISPLACEMENT OF PIPE, MACHINE AND SPRINGS

Fig. 1. Schematic of pipe loading configuration.

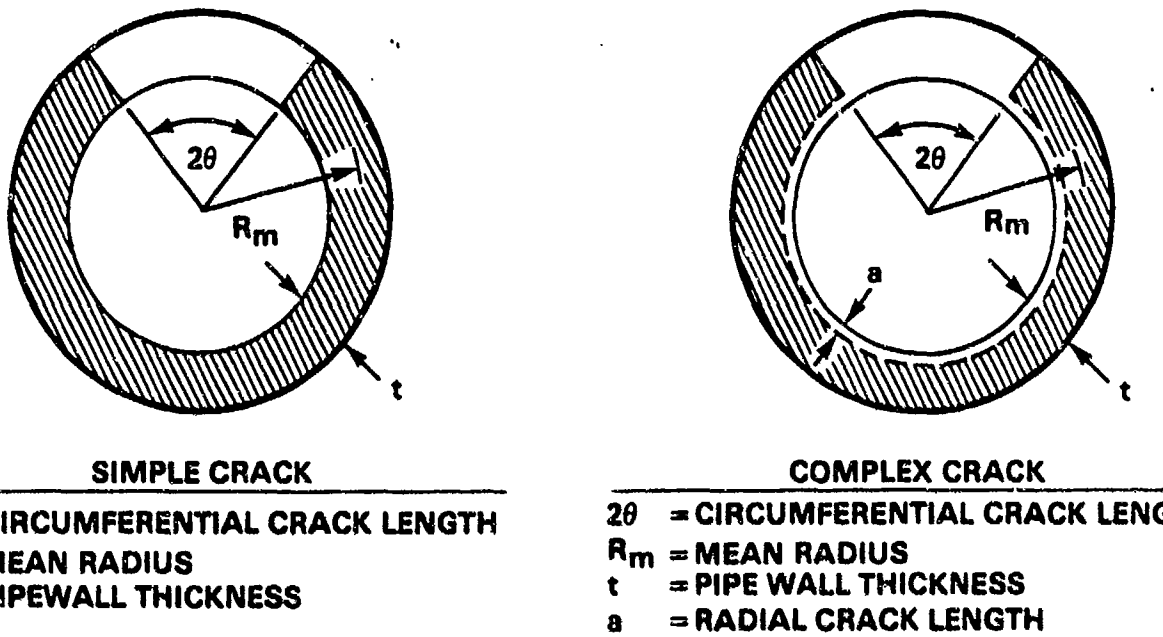

Fig. 2. Simple and complex crack geometries.

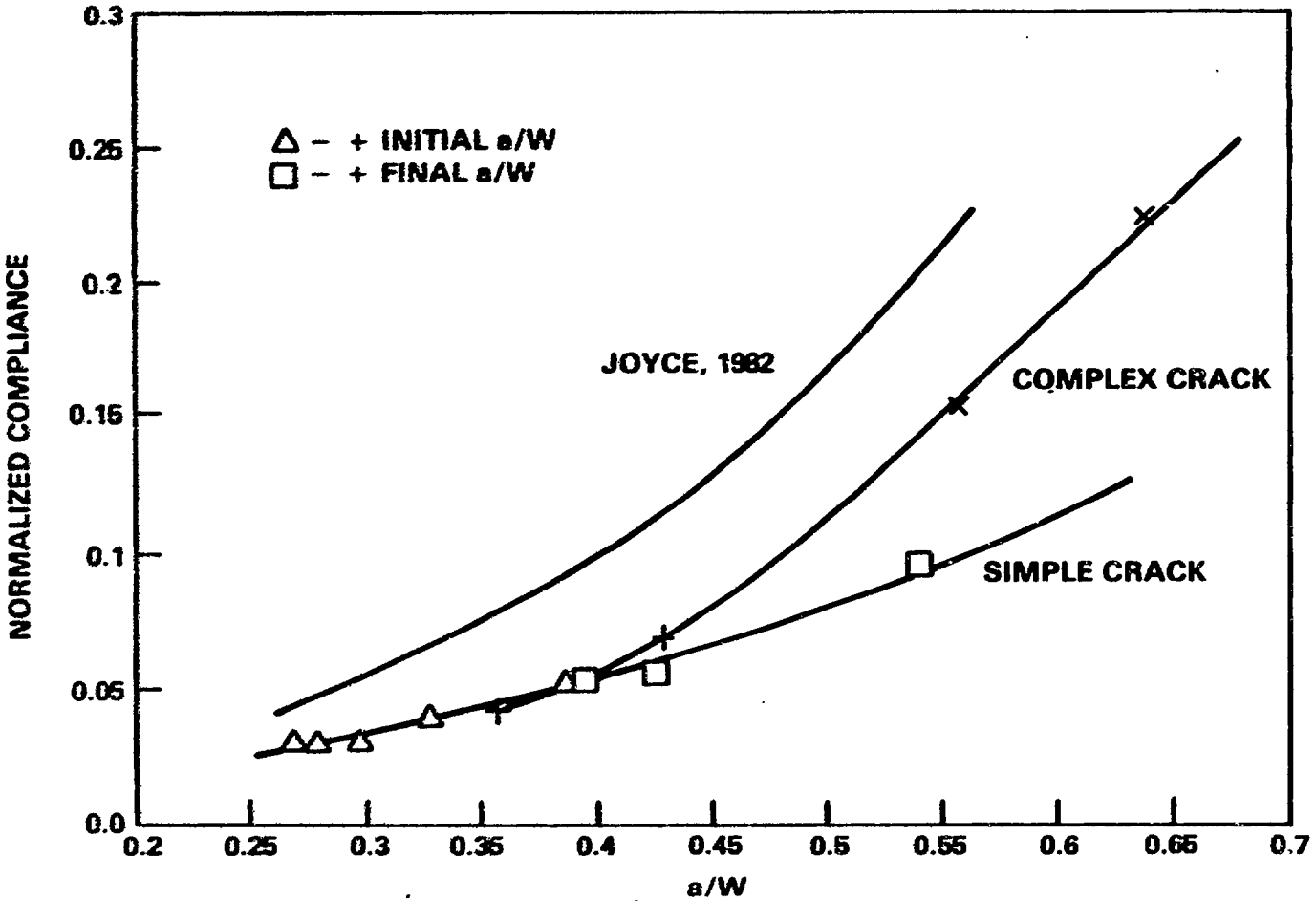

Fig. 3. Elastic compliance calibration curve for pipe geometries.

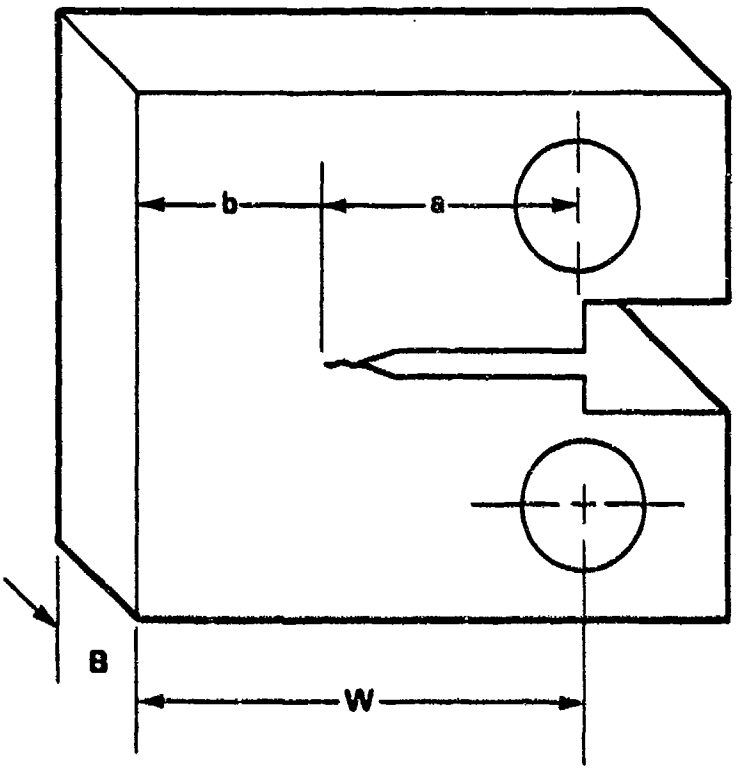

Fig. 4. Compact tension specimen design.

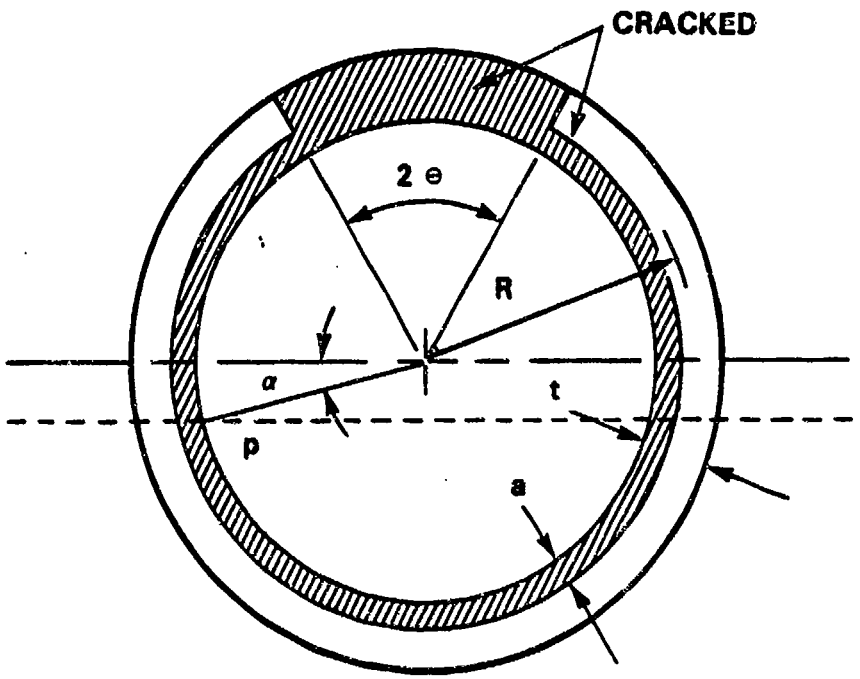

Fig. 5. Pipe crack cross-section showing limit load parameters.

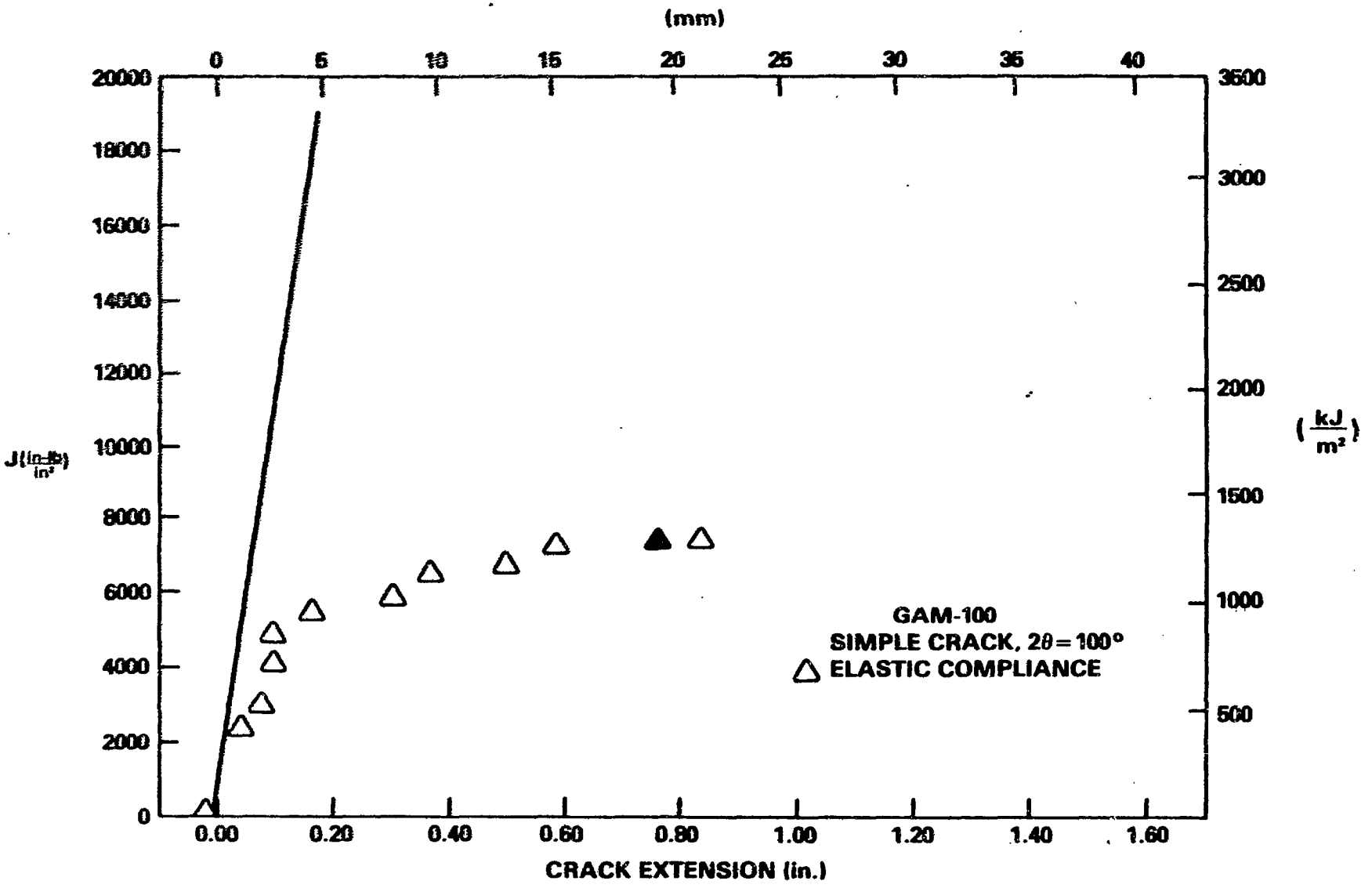

Fig. 6. J-R curve results for pipe specimen GAM-100 (simple crack geometry).

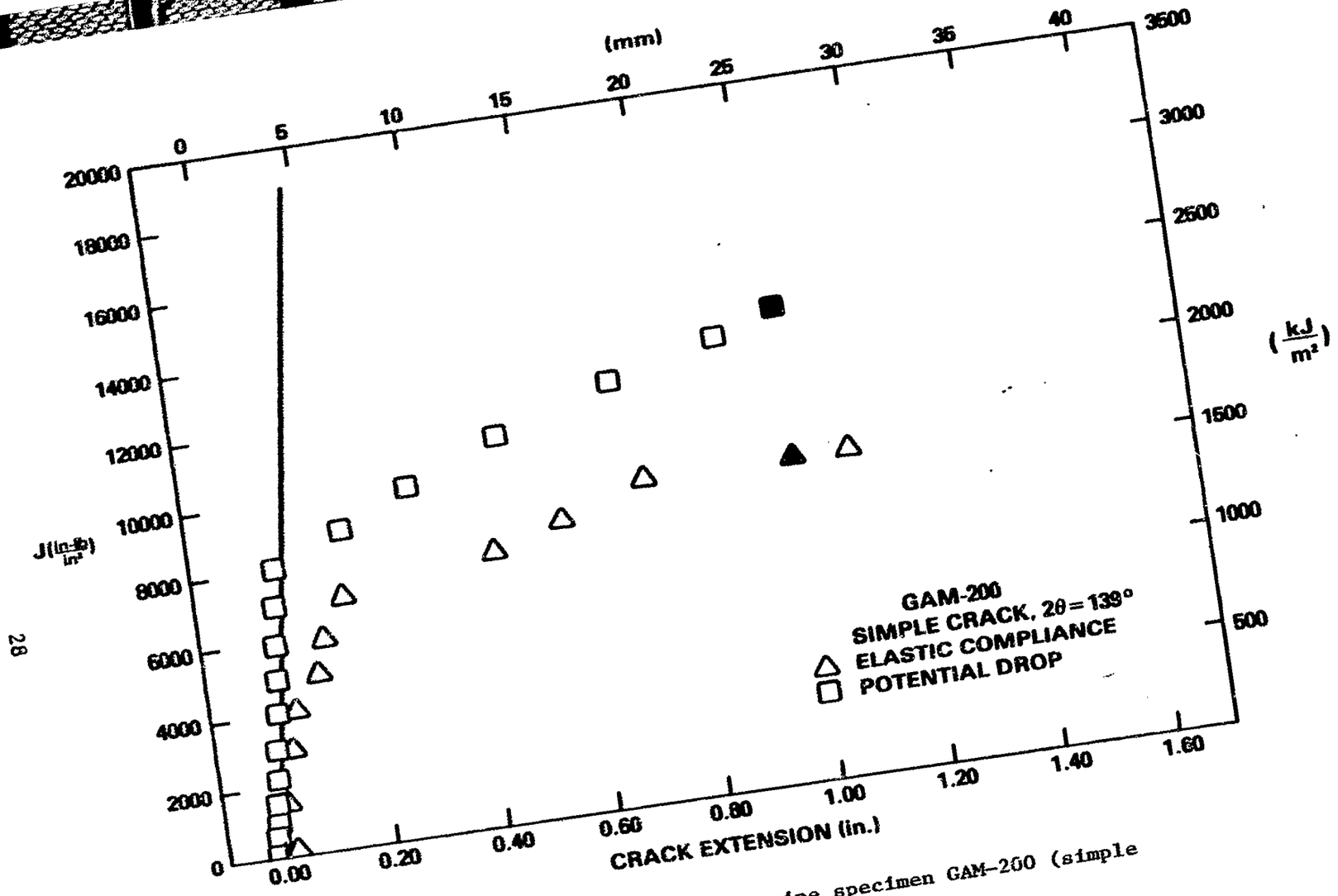

Fig. 7. J-R curve results for pipe specimen GAM-200 (simple crack geometry).

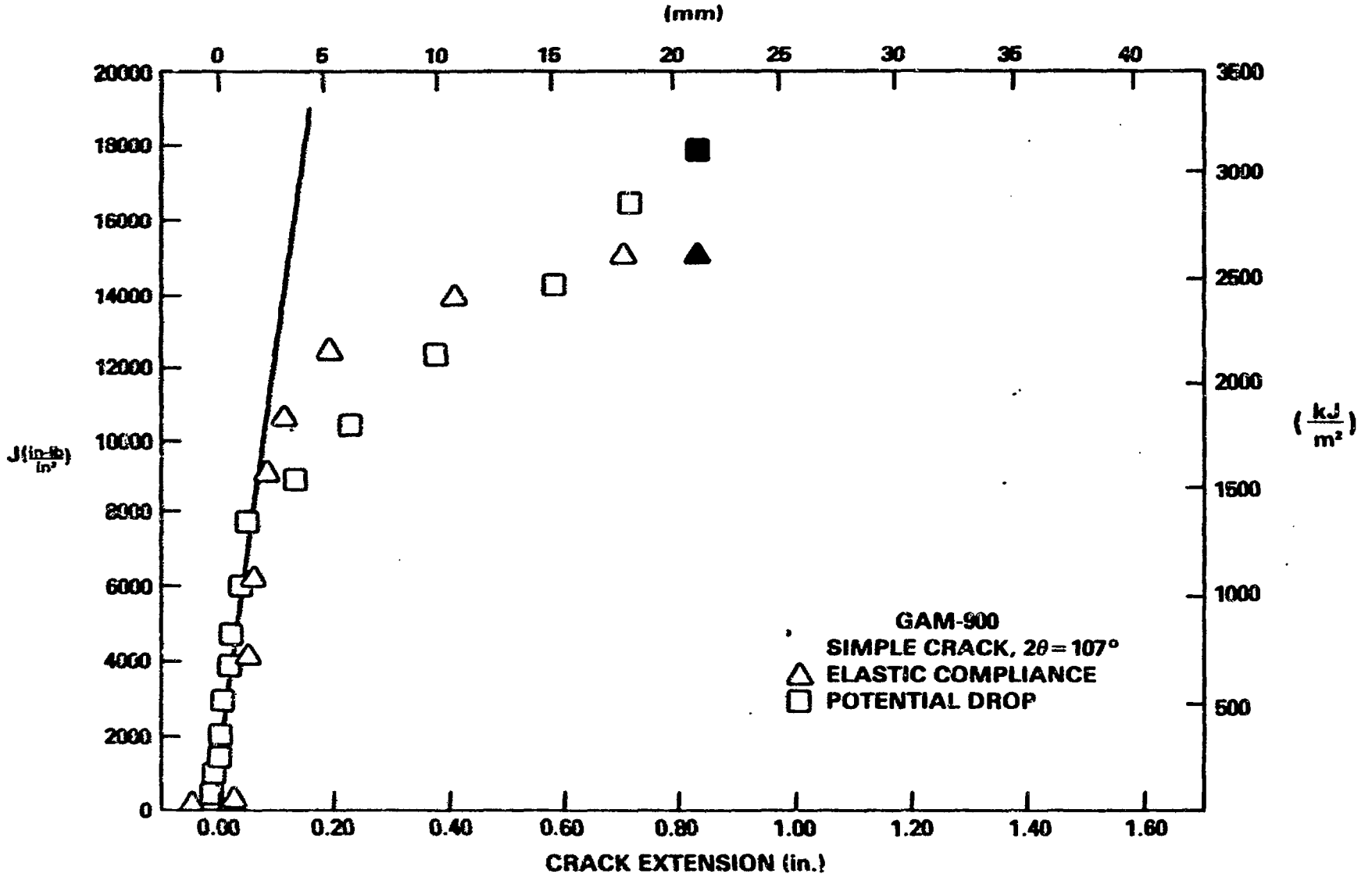

Fig. 8. J-R curve results for pipe specimen GAM-900 (simple crack geometry).

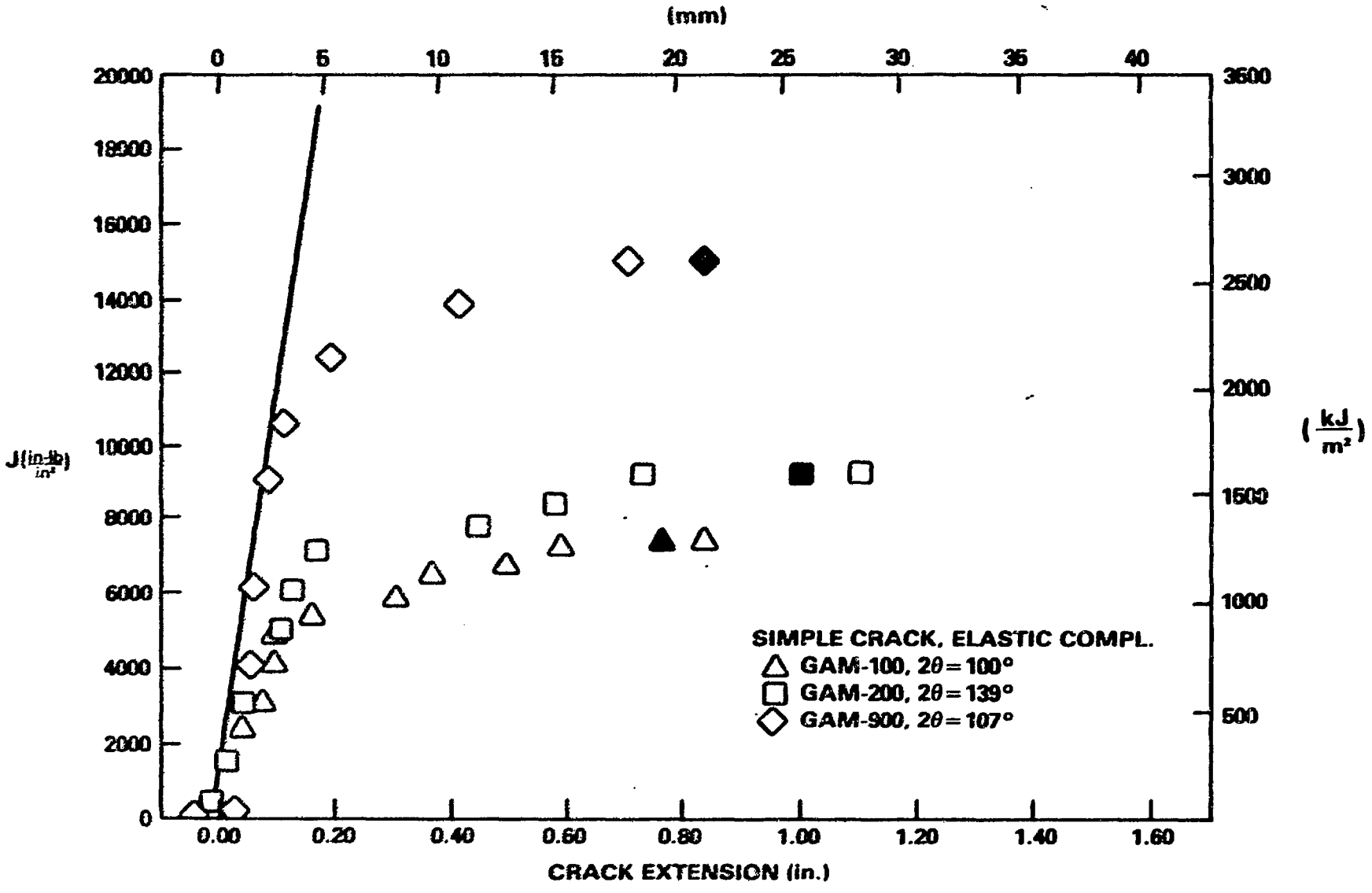

Fig. 9. Comparison of J-R curves for pipe specimens containing simple crack geometry from elastic compliance.

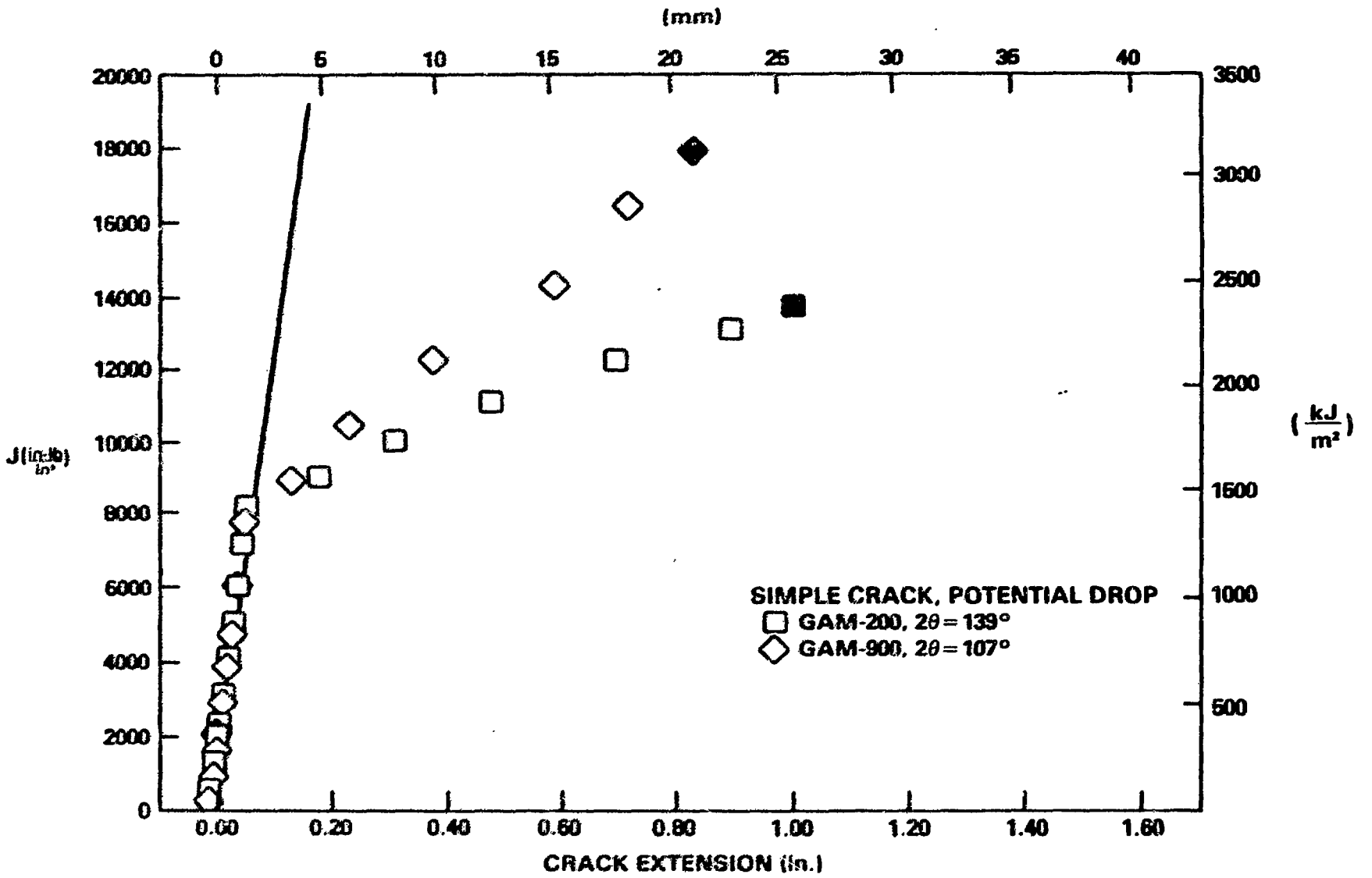

Fig. 10. Comparison of J-R curves for pipe specimens containing simple crack geometry from DC potential drop.

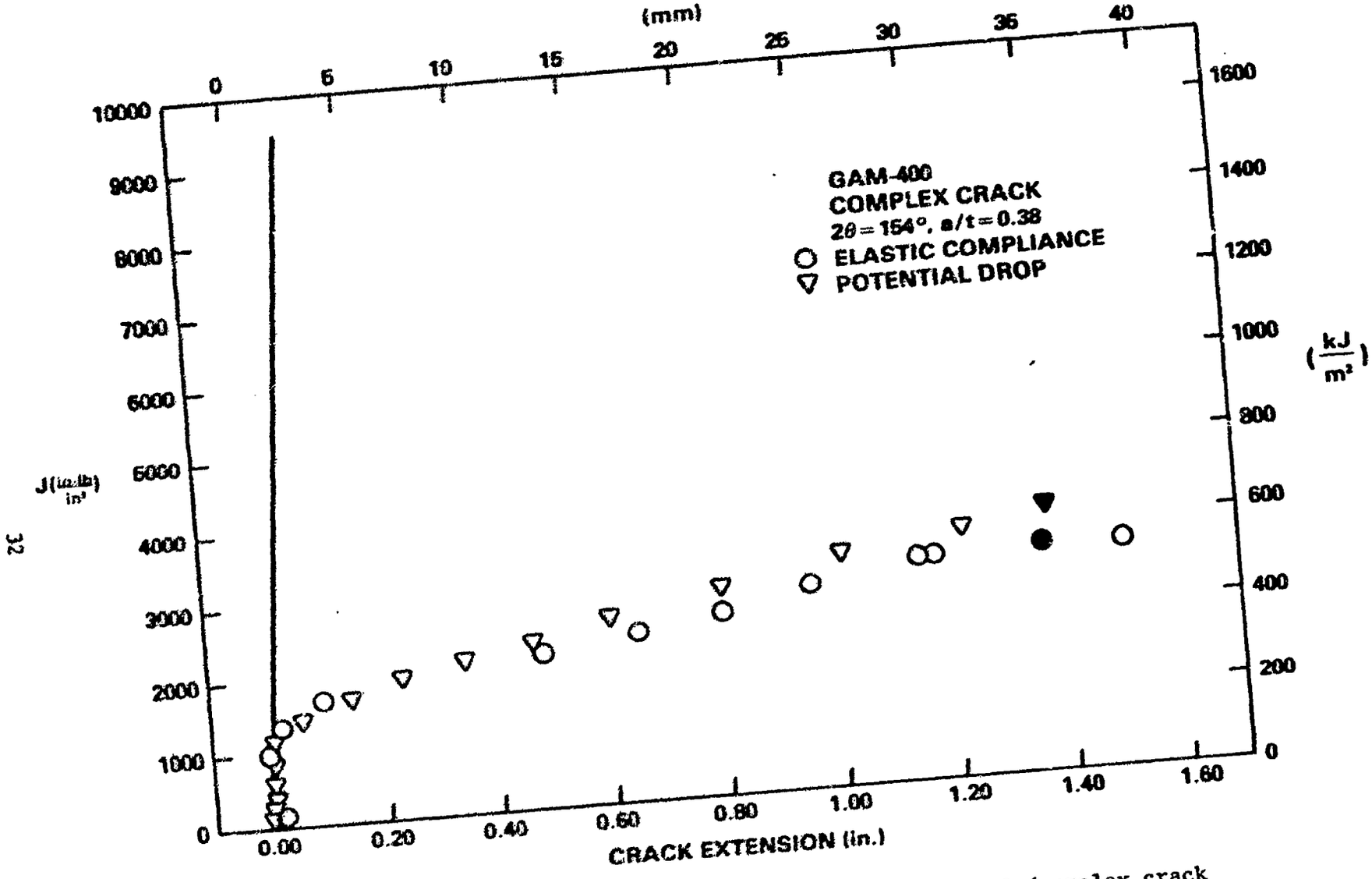

Fig. 11. J-R curve results for pipe specimen GAM-400 (complex crack geometry).

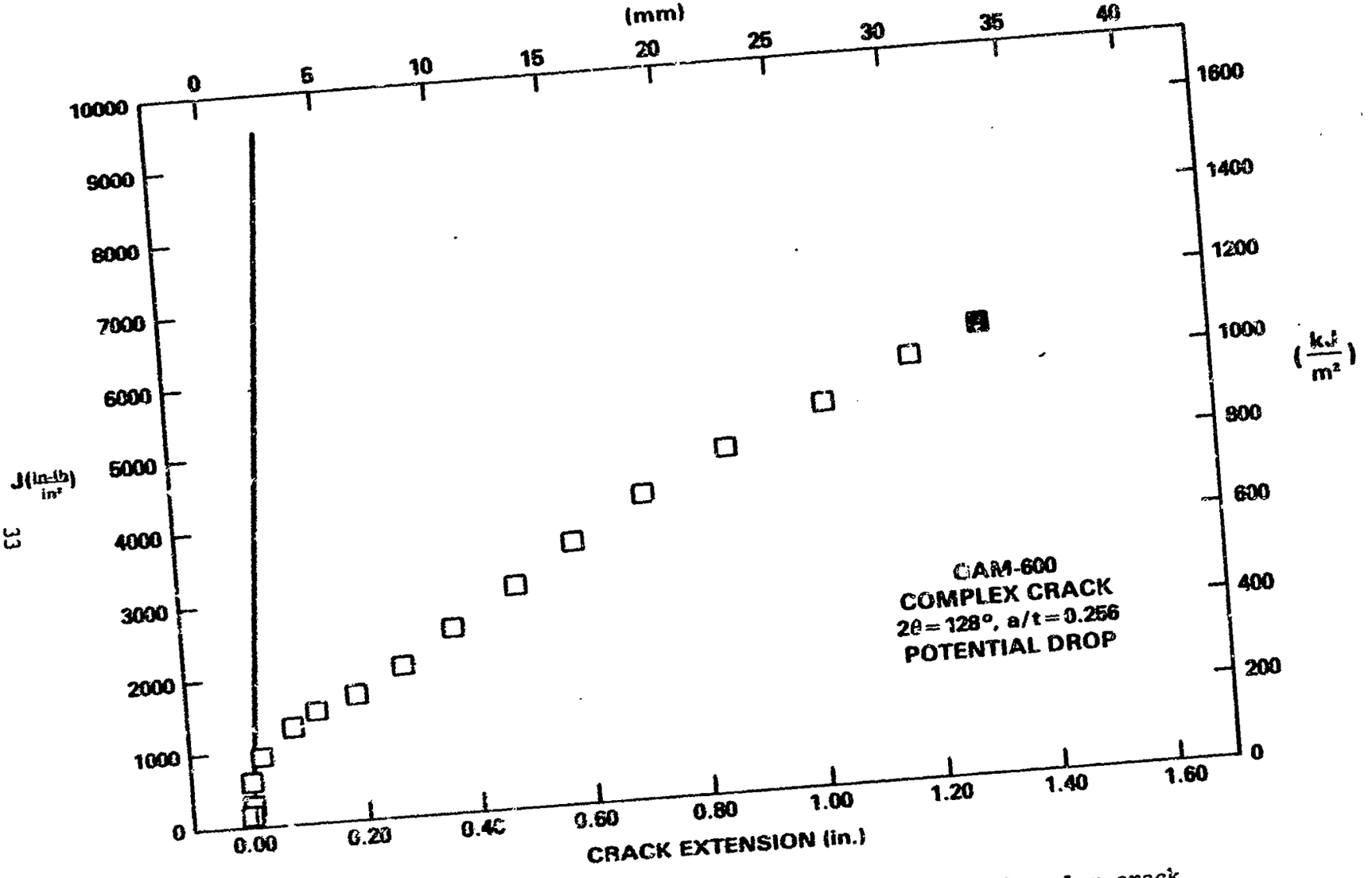

Fig. 12. J-R curve results for pipe specimen GAM-600 (complex crack geometry).

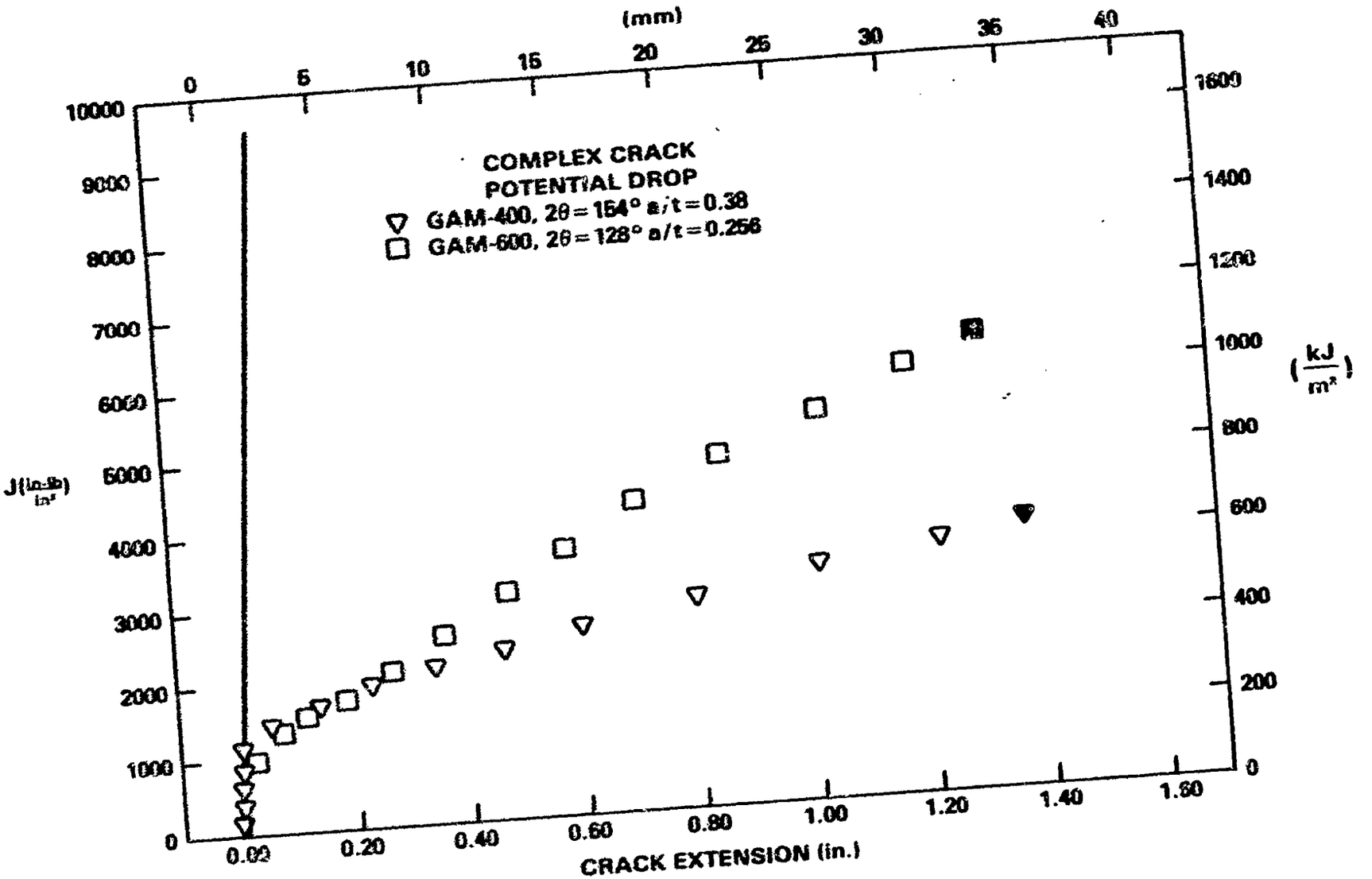

Fig. 13. Comparison of J-R curves for pipe specimens containing complex crack geometry from DC potential drop.

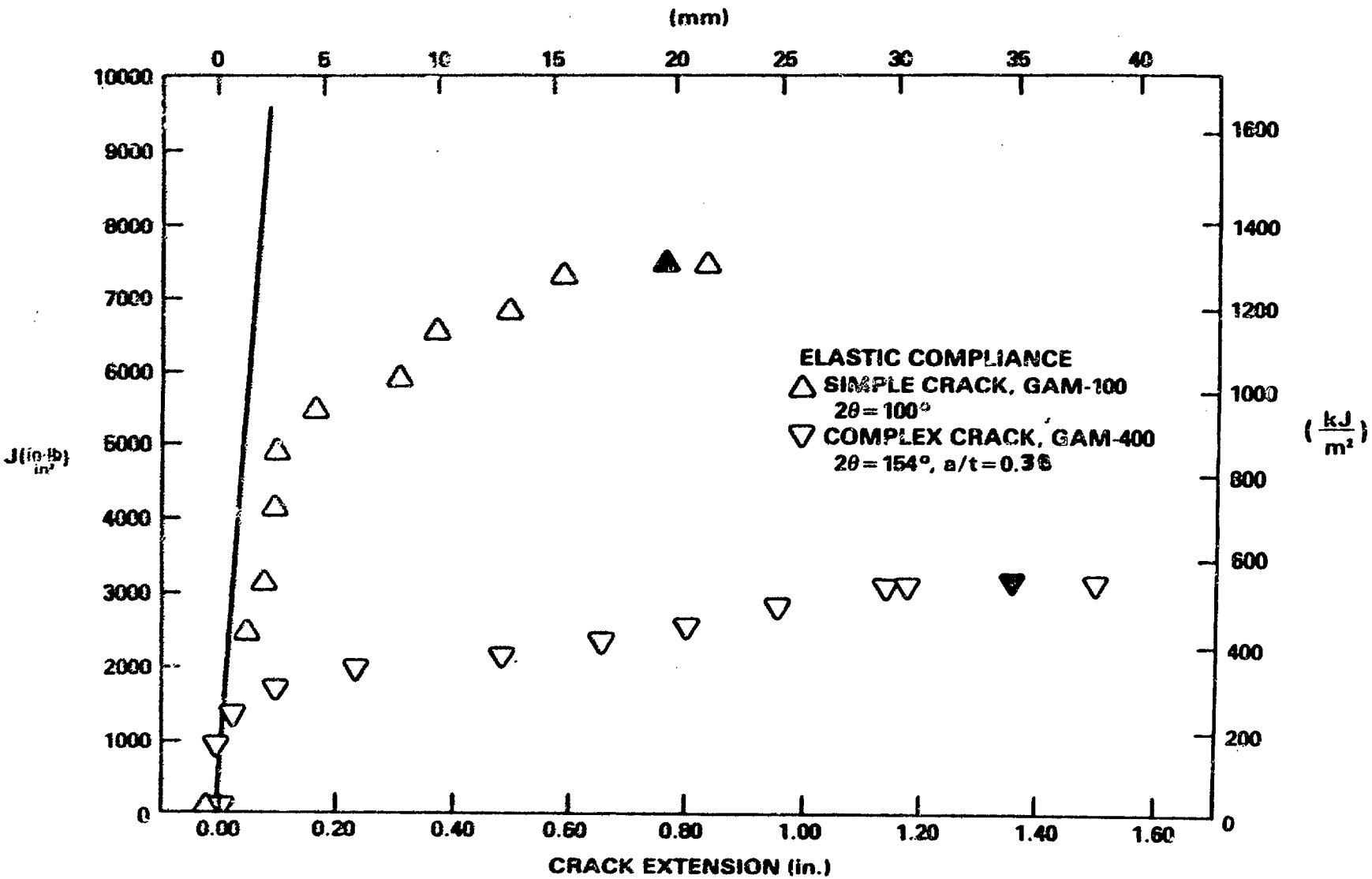

Fig. 14. Comparison of J-R curves for pipes containing simple and complex crack geometries from elastic compliance.

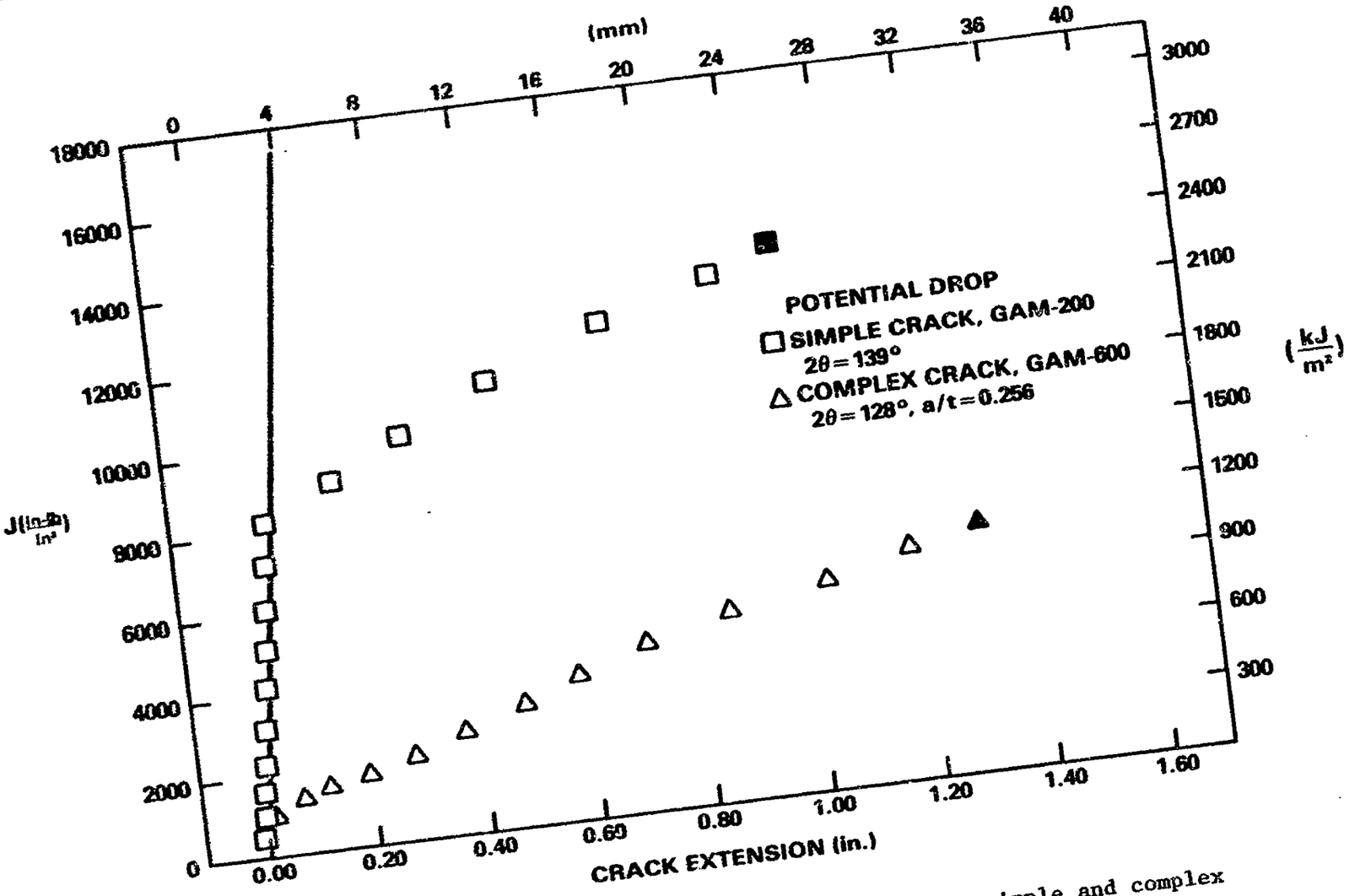

Fig. 15. Comparison of J-R curves for pipes containing simple and complex crack geometries from DC potential drop.

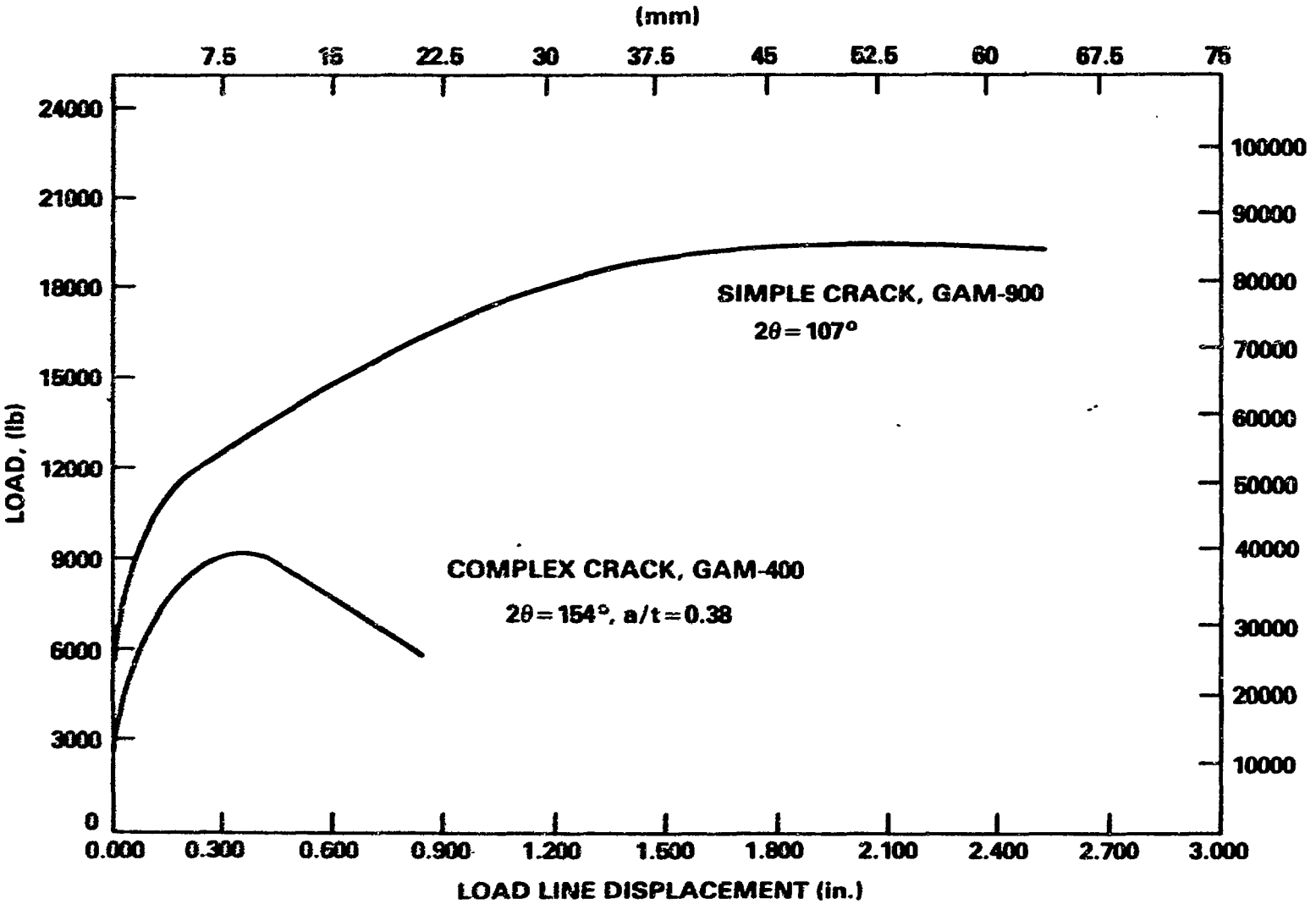

Fig. 16. Load versus displacement records from pipes containing simple and complex cracks.

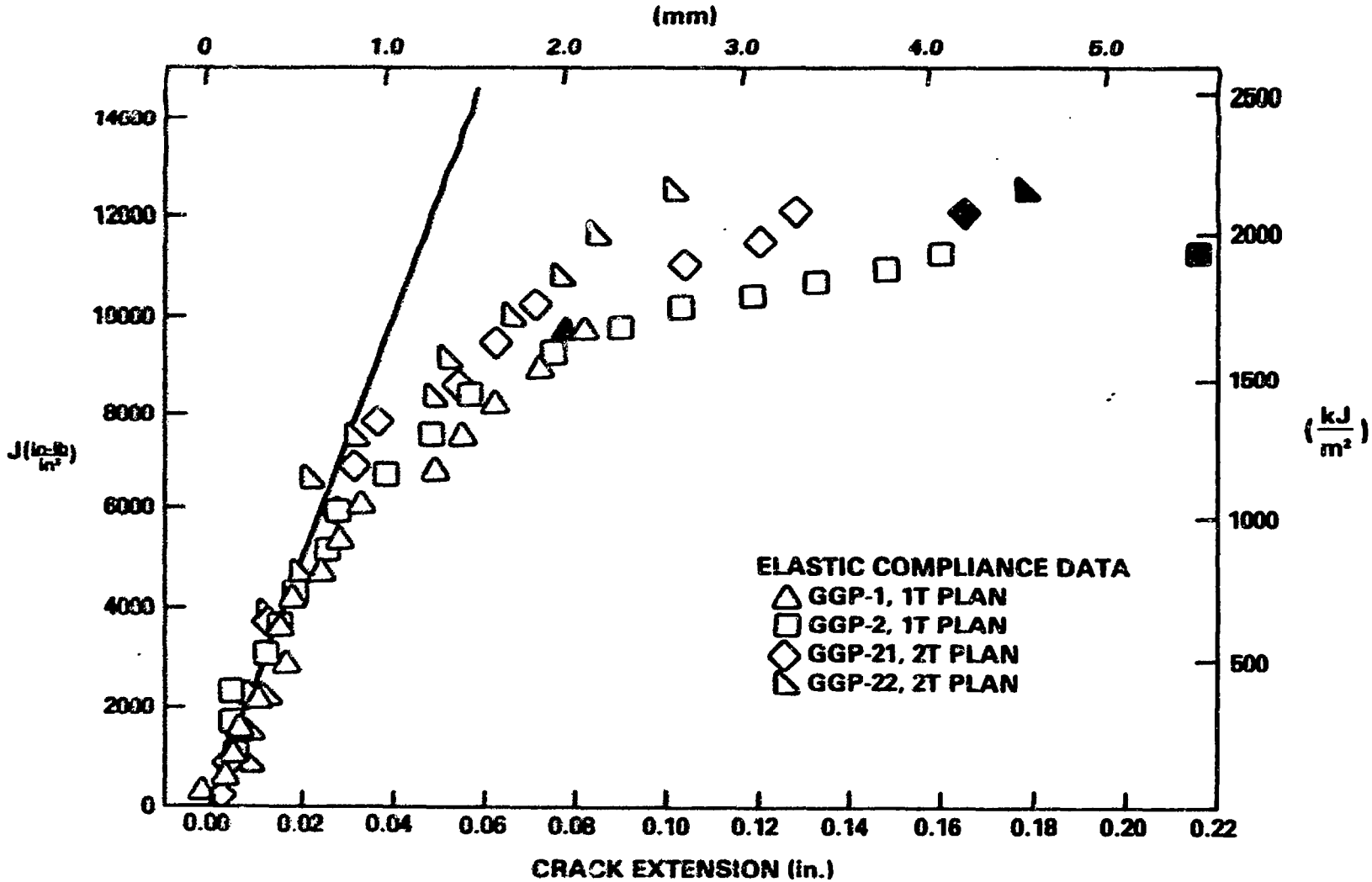

Fig. 17. J-R curve results for 1T and 2T plan compact tension specimens from elastic compliance.

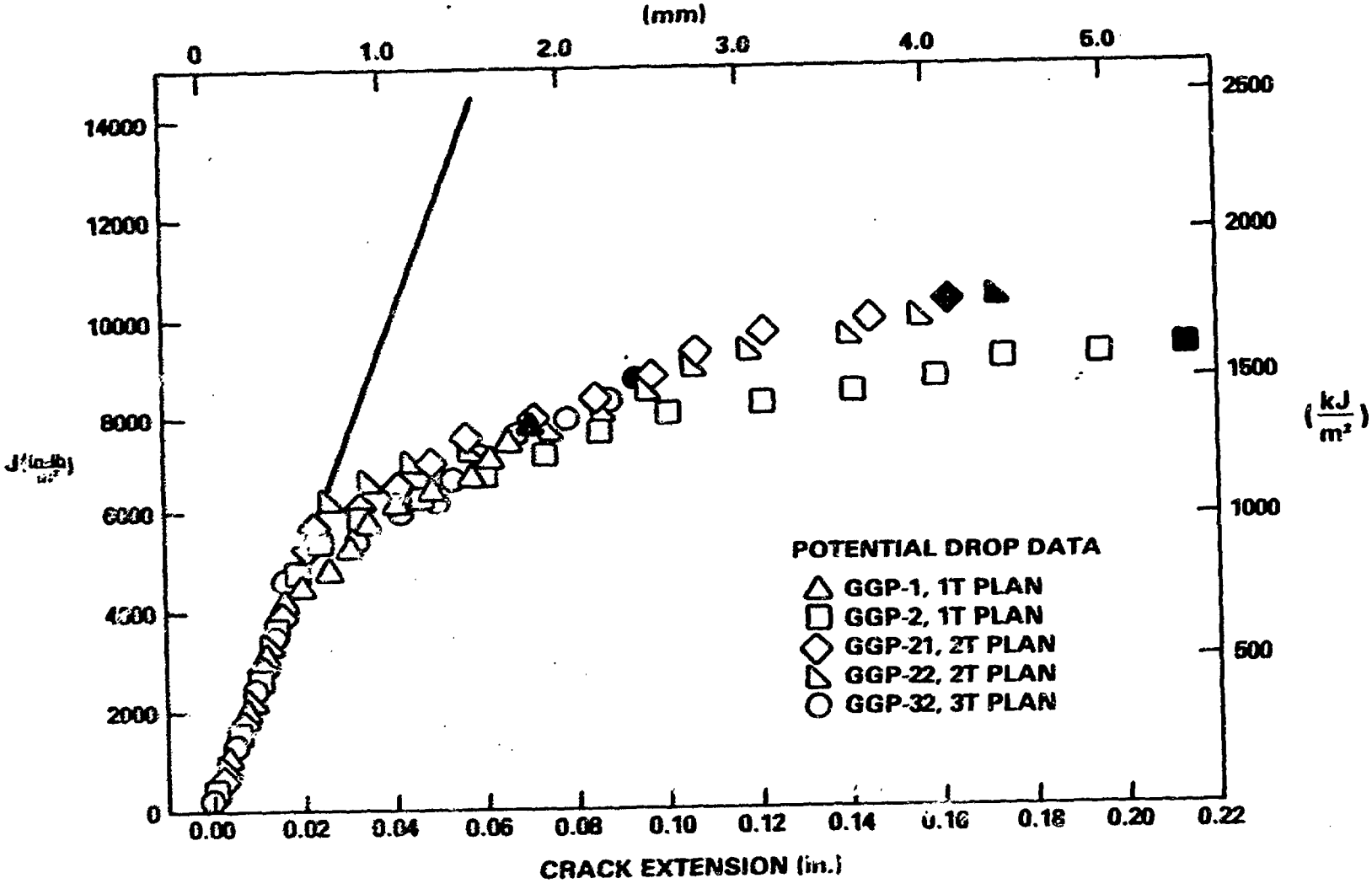

Fig. 18. J-R curve results for 1T, 2T, and 3T plan compact tension specimens from DC potential drop.

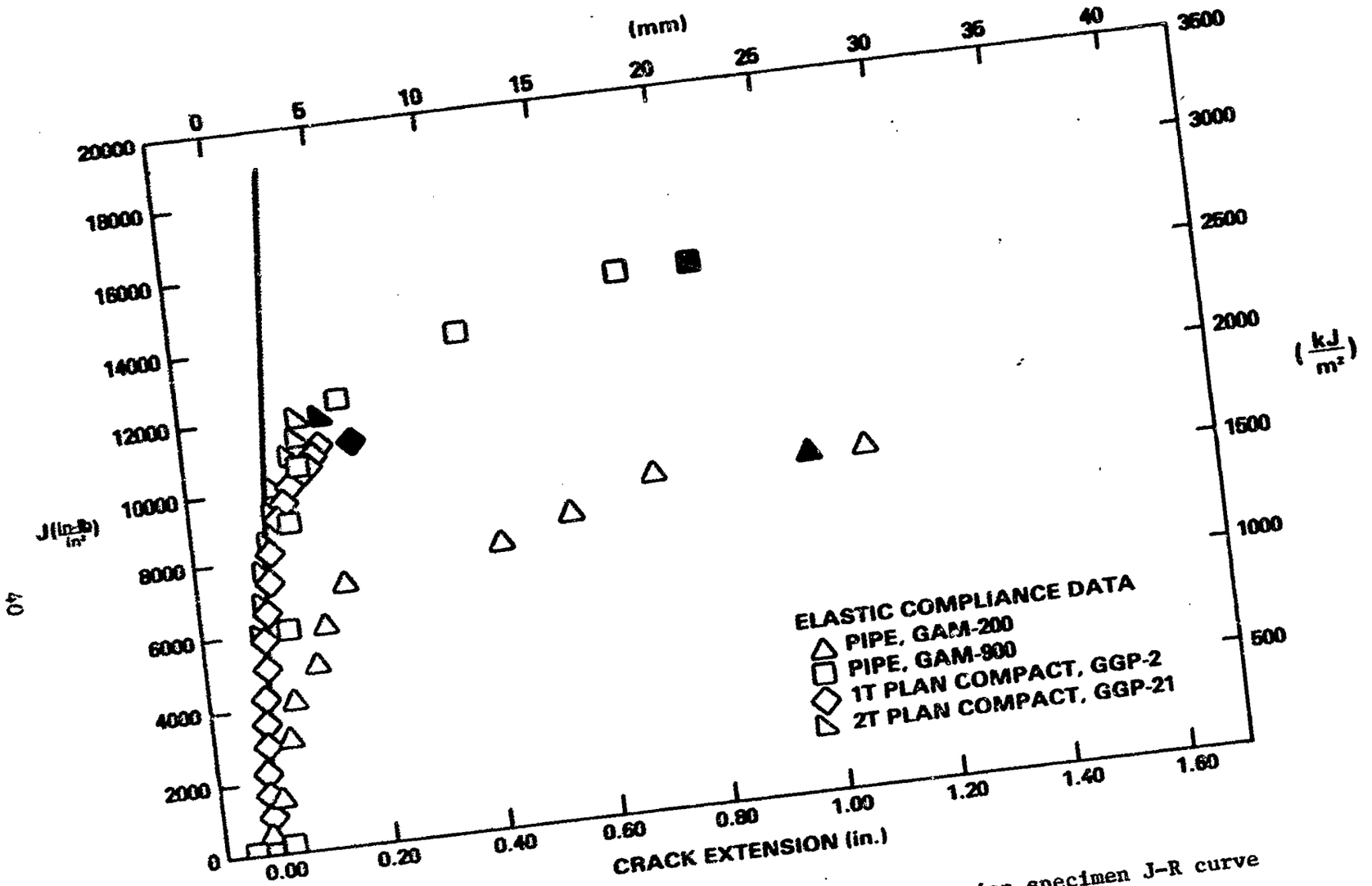

Fig. 19. Comparison of pipe specimen and compact tension specimen J-R curve results from elastic compliance.

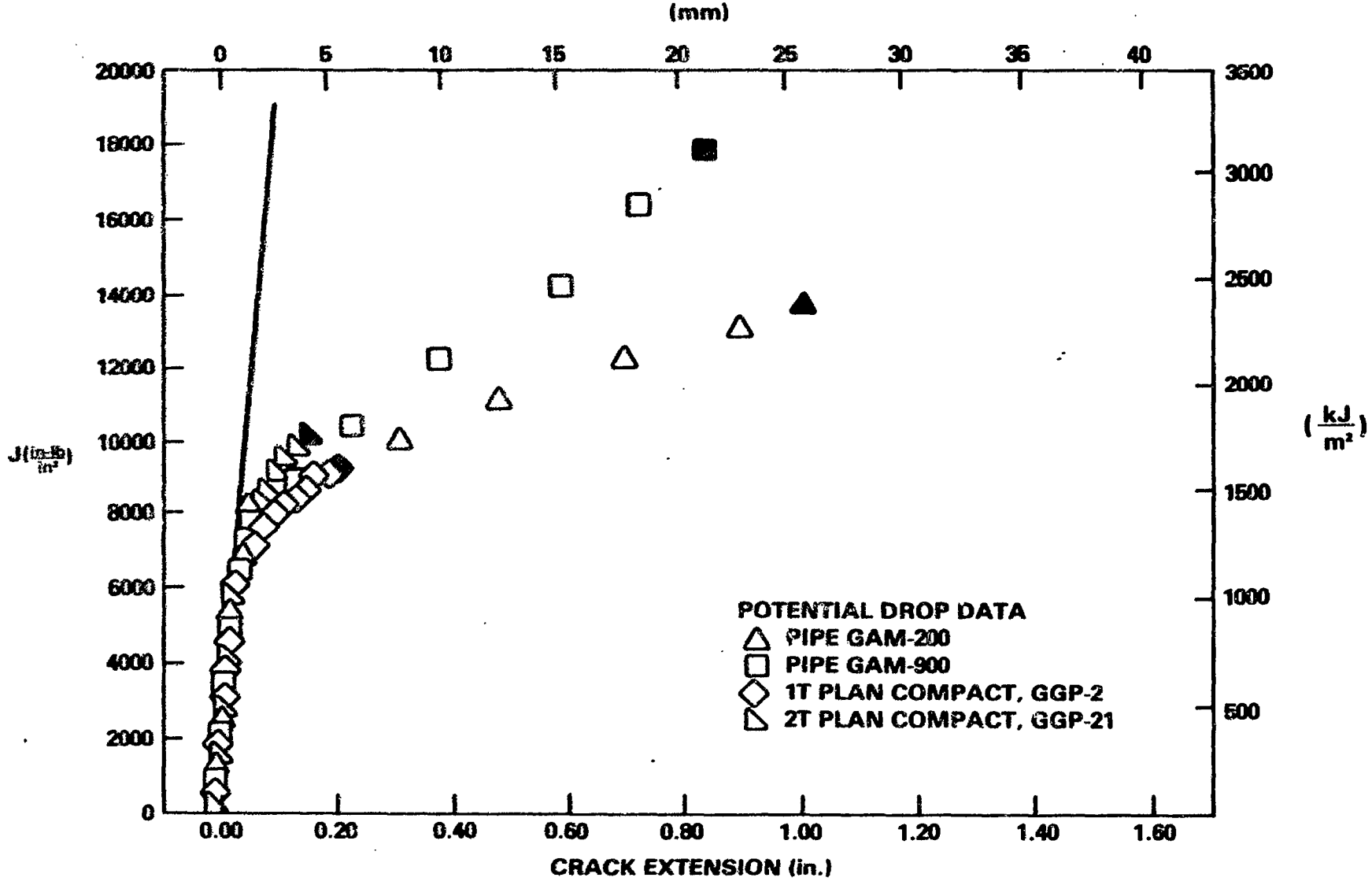

Fig. 20. Comparison of pipe specimen and compact tension specimen J-R curve results from DC potential drop.

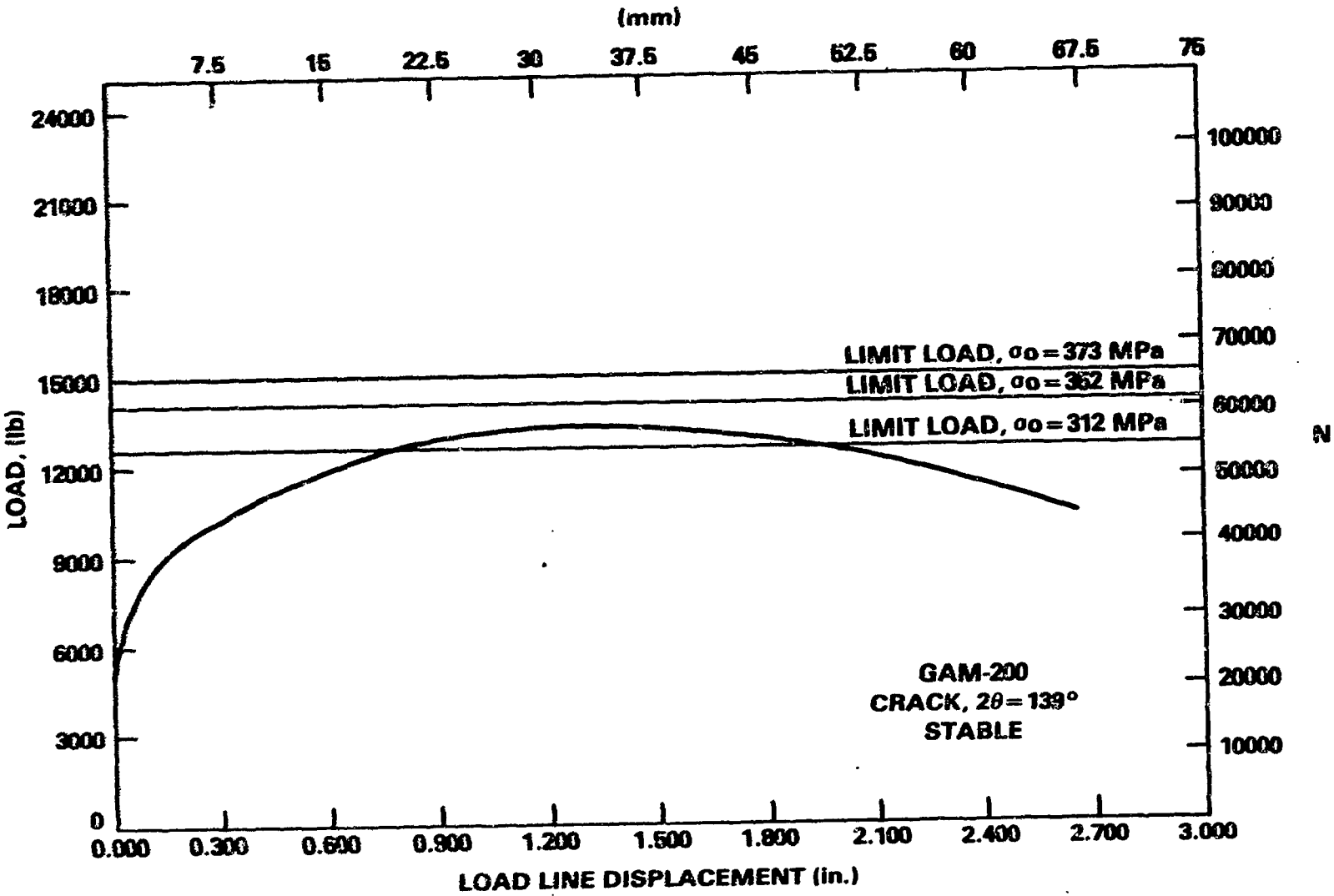

Fig. 21. Limit load results for pipe specimen GAM-200 (simple crack geometry).

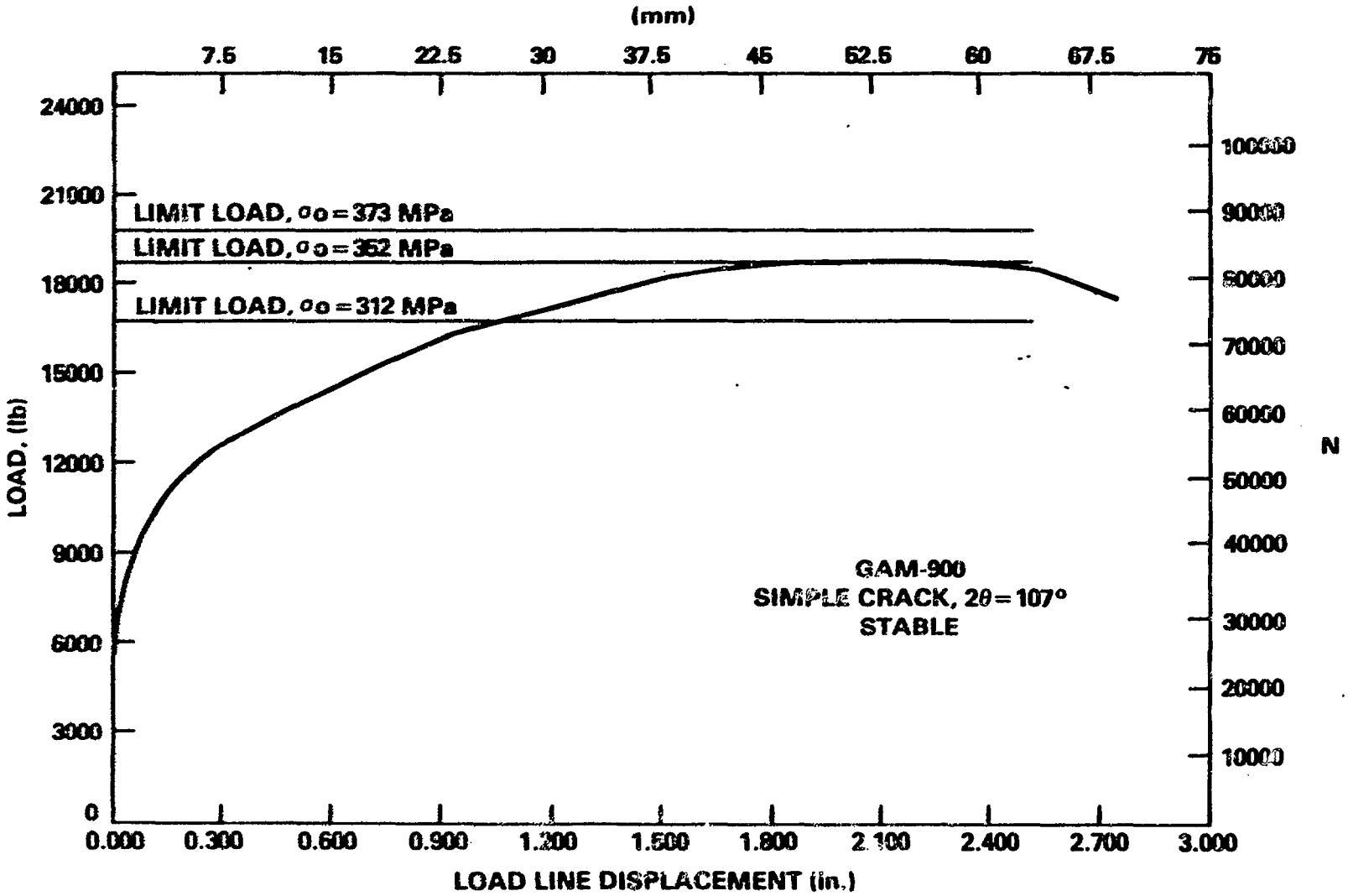

Fig. 22. Limit load results for pipe specimen GAM-900 (simple crack geometry).

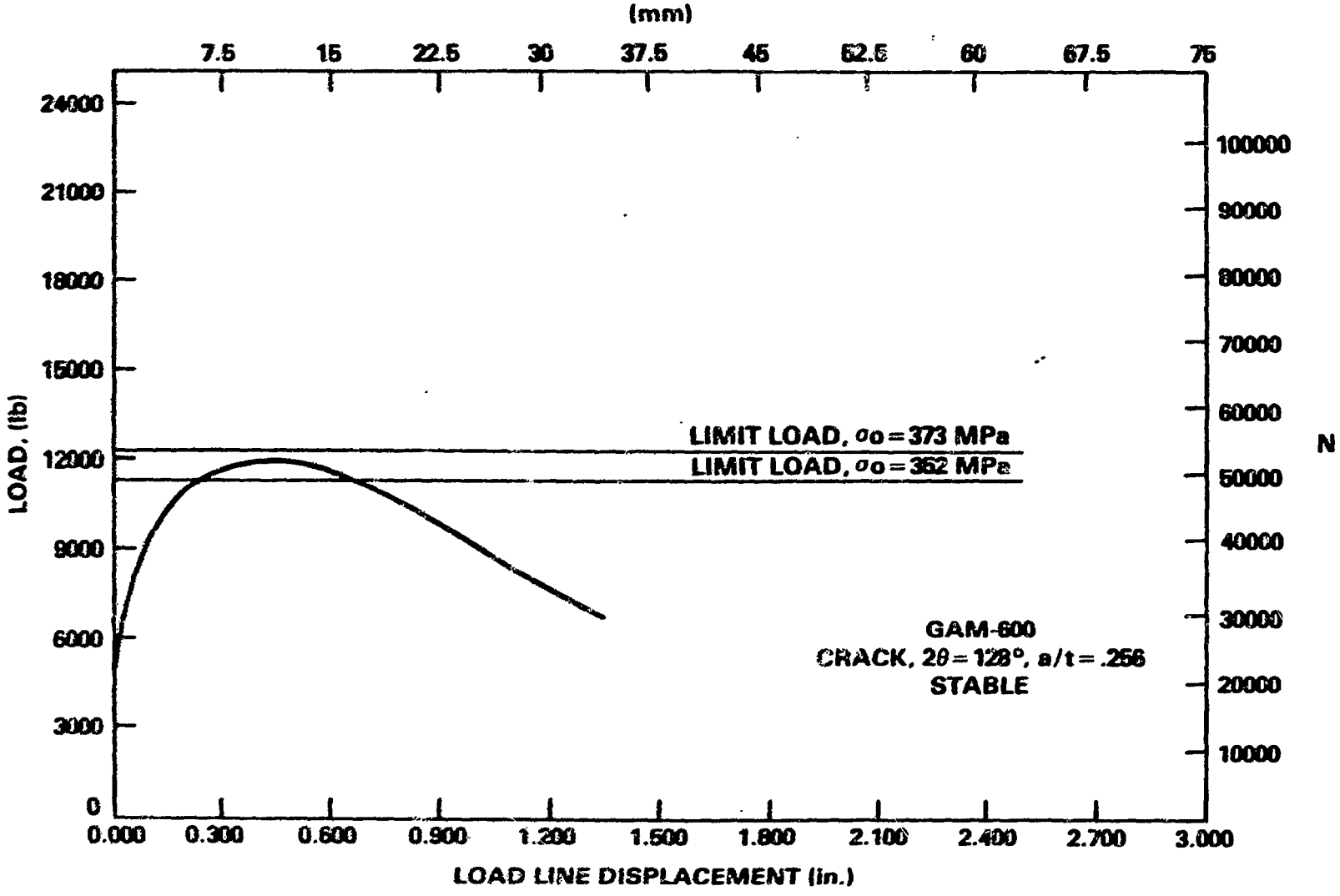

Fig. 23. Limit load results for pipe specimen GAM-600 (complex crack geometry).

REFERENCES

1. Wilkowski, G.M., A. Zahoor, M.F. Kanninen, "A Plastic Fracture Mechanics Prediction of Fracture Instability in a Circumferentially Cracked Pipe in Bending-Part II: Experimental Verification on a Type 304 Stainless Steel Pipe", Journal of Pressure Vessel Technology, Vol. 103, November 1981.

2. Vassilaros, M.G., R.A. Hays, J.P. Gudas, J.A. Joyce, "J-integral Tearing Instability Analyses for 8 in. Diameter ASTM A106 Steel Pipe", NUREG/CR 3740, U.S. Nuclear Regulatory Commission Report, April 1984.

3. Bruckner, A., R. Grunmach, B. Kneiffel, D. Munz, G. Thun, "Fracture of Pipes with Through-Wall Circumferential Cracks in Four Point Bending", Circumferential Cracks in Pressure Vessels and Piping- Vol. II - PVP-Vol. 95, Editor: G.M. Wilkowski, ASME.

4. American Society of Mechanical Engineers Boiler and Pressure Vessel Code, Section XI IWB-3640 (Winter Addenda 1983).

5. Ranganath, S., and H.S. Mehta, "Engineering Methods for the Assessment of Ductile Fracture Margin in Nuclear Power Plant Piping", Elastic Plastic Fracture Second Symposium, Vol. 2, "Fracture Resistance Curves and Engineering Applications", ASTM STP 803, American Society for Testing and Materials, Philadelphia, PA, 1983.

6. "Mechanical Fracture Predictions for Sensitized Stainless Steel Piping with Circumferential Cracks", EPRI Report NP-192, Final Report, Electric Power Research Institute, Palo Alto, CA, Sept 1976.

7. "Review and Assessment of Research Relevent to Design Aspects of Nuclear Power Plant Piping Systems", NUREG-0307, Nuclear Regulatory Commission, Washington, D.C., July 1977.

8. Joyce, J.A., "Instability Tests of Compact and Pipe Specimens Utilizing a Test System Made Compliant by Computer Control", NUREG/CR-2257, U.S. Nuclear Regulatory Commission Report, March 1982.

9. Vassilaros, M.G. and E.M. Hackett, "J-Integral R-Curve Testing of High Strength Steel Utilizing the D.C. Potential Drop Method", ASTM 15th National Symposium on Fracture Mechanics, ASTM STP 833.

10. Wilkowski, G.M., and W.A. Maxey, "Applications of the Electrical Potential Method for Measuring Crack Growth in Specimens, Flawed Pipes and Pressure Vessels", ASTM 14th National Symposium on Fracture Mechanics, ASTM STP 791.

11. Joyce, J.A., and J.P. Gudas, "Elastic-Plastic Fracture", ASTM STP 668, J.D. Landes, J.A. Begley, and G.A. Clarke, Eds., American Society for Testing and Materials, 1979, pp. 251-265.

12. Ernst, H.A., P.C. Paris, and J.D. Landes, "Estimations on J-Integral and Tearing Modulus T from a Single Specimen Test Record", ASTM STP 743, R. Roberts Ed., American Society of Testing and Materials, 1981.

13. Zahoor, A., and M.F. Kanninen, "A Plastic Fracture Mechanics Prediction of Fracture Instability in a Circumferentially Cracked Pipe in Bending - Part I: J-Integral Analysis", ASME, J. of Pressure Vessel Technology, Vol. 103, Number 4, Nov 1981.

14. Tada, H., P.C. Paris, and R. Gamble, "Stability Analysis of Circumferential Cracks in Reactor Piping Systems", U.S. Nuclear Regulatory Commission Report, NUREG/CR-0838, June 1976.

15. Wilkowski, G.M., et al., "Degraded Piping Program-Phase II Semiannual Report October 1984 - March 1985", Nuclear Regulatory Commission Report, NUREG/CR-4082 Vol. 2, July 1985.

16. Smith, E., "The Geometry Dependence of the J-R Curve for Circumferential Growth of Through-Wall Cracks in Cylindrical Pipes Subject to Bending Loads", Engineering Fracture Mechanics, Vol 18, No. 6, pp 1119-1123, Pergamon Press Ltd., 1983.

INITIAL DISTRIBUTION

Copies		
2	ONR	
	1	1131M
	1	1132SM
4	NRL	
	1	6000
	1	6320
	1	6380
	1	6396
12	NAVSEA	
	1	SEA 05D
	2	SEA 05R
	1	SEA 08
	1	SEA 092
	2	SEA 323
	1	PMS 393
	1	PMS 395
	1	PMS 396
	2	SEA 99612
1	NISC Code 369	
12	DTIC	

CENTER DISTRIBUTION

Copies	Code	Name
1	17	M. Krenzke
1	173	A.B. Stavovy
1	1720.1	T. Tinley
1	28	G. Wacker
1	2802	
1	2803	J. Cavallaro
1	2809	A. Malec
5	281	J. Gudas
10	2814	T. Montemarano
1	522.2	Unclass. Lib.
2	5231	Office Services

DTNSRDC ISSUES THREE TYPES OF REPORTS:

1. **DTNSRDC reports, a formal series,** contain information of permanent technical value. They carry a consecutive numerical identification regardless of their classification or the originating department.

2. **Departmental reports, a semiformal series,** contain information of a preliminary, temporary, or proprietary nature or of limited interest or significance. They carry a departmental alphanumerical identification.

3. **Technical memoranda, an informal series,** contain technical documentation of limited use and interest. They are primarily working papers intended for internal use. They carry an identifying number which indicates their type and the numerical code of the originating department. Any distribution outside DTNSRDC must be approved by the head of the originating department on a case-by-case basis.